Reply to referee's comments

22 September 2016

General comments

We thank all reviewers for their comments, leading to an improvement of our manuscript. We collected some general comments, since some issues were addressed by all reviewers.

Restructuring of the manuscript

We restructured the manuscript in the following way:

- We generally revised the text to avoid misunderstanding, following many suggestions of the reviewers.
- We have shortened the derivation of the model and put the details into appendix B.
- We expanded the analysis part as well as the description of the analysis tools.
- We also expanded our comparison of the model results with observations in order to address the topic "subvisible cirrus clouds" adequately.

Dry adiabatic motion, latent heat release, temperature/velocity regime

If latent heat release was taken into account for the rate of RH_i, the temperature equation (18) would read

$$\frac{\mathrm{d}T}{\mathrm{d}t} = \frac{\mathrm{d}T}{\mathrm{d}z}\frac{\mathrm{d}z}{\mathrm{d}t} + \left.\frac{\mathrm{d}T}{\mathrm{d}t}\right|_{\text{latheat}} = -\frac{g}{cp}w + \frac{L_{ice}}{M_{air}c_p}\cdot\left.\frac{\mathrm{d}q_c}{\mathrm{d}t}\right|_{\text{growth}}, \tag{1}$$

and the latent heat term would need to be included in the rate equation for RH_i:

$$\frac{\mathrm{d}RH_i}{\mathrm{d}t} = \underbrace{e\cdot w\cdot RH_i}_{\text{adiabatic}} - \left.\frac{\mathrm{d}q_c}{\mathrm{d}t}\right|_{\text{growth}}\left(\underbrace{\frac{p}{\varepsilon p_{si}(T)}\cdot 100\%}_{\text{growth}} - \underbrace{RH_i\frac{L_{ice}^2}{RT^2M_{air}c_p}}_{\text{latent heat}}\right). \tag{2}$$

The contribution to temperature change from latent heat is obviously only important, when there is substantial diffusional growth of ice particles, i.e. when $\frac{\mathrm{d}q_c}{\mathrm{d}t}|_{\mathrm{growth}}$ is considerably large. In that case however, the latent heat term directly competes with the growth term. The growth term is usually at least one order of magnitude larger than the latent heat term. Hence, whenever latent heat release comes into play for temperature changes, the rate of change of RH_i is dominated by the water vapour sink due to growth, anyway. Therefore, we omit latent heating in the RH_i equation and stick with the constant adiabatic forcing term. Including latent heating would produce an additional highly nonlinear term (it contains RH_i as a factor), which we would like to avoid.
In terms of lapse rates we can state that due to phase changes a "moist" (or better "ice") adiabatic lapse rate might be more appropriate. However, since we investigate cirrus clouds in the low temperature regime $T < 235\,\mathrm{K}$, the difference between moist adiabatic lapse rate and dry adiabatic lapse rate is less than 5% and decreases with decreasing temperature. Thus, we can approximate the temperature change by adiabatic lapse rate and omit the additional nonlinear term. This is also noted in the text.
We also describe the relevant regime for SVCs, i.e. low temperatures $T < 235\,\mathrm{K}$ and slow vertical updraughts $w < 0.05\,\mathrm{m\,s^{-1}}$ in the first part of the manuscript.

Terminology

We changed the term "(positive) attractor" to "(positive) point attractor" or "stable focus" for clarity. We use the term "critical point" according to Verhulst [1996], which is equivalent to "steady state" or "equilibrium point". We add some information that the limit cycle is a one-dimensional attractor.

Response to Peter Nevier

Boltzmann equation The evolution equation of the size distribution has a form that is similar to the Boltzmann equation (e.g. in gas dynamics). However, since we have no aggregation terms on the right hand side, we follow the suggestions and omit this name.

Eulerian vs. Lagrangian description Since we are interested in the time evolution of an air parcel, the change from Eulerian to Lagrangian description seems reasonable. We added more details for the transformation of the equations; especially, we describe the reformulation of the evolution equation in advective form, using mass conservation of air (appendix A).

ODE system We write the equation in a simpler way, using constants in order to represent the essential non-linear features of the equations. We added a paragraph for a qualitative description of the different terms (non-linear/linear, etc.) and calculated the divergence for determining the quality of the system (externally forced dissipative system).

Spelling We corrected all typos, especially the names of the physicists and mathematicians Euler and Lagrange.

Response to reviewer #1

Major comments

L252–256 See general comments.

L363–364 As it is a limit cycle, it takes infinitely long for the orbit to reach it. However, in the numerical solution, the oscillation amplitude stays approximately constant after several periods. This is apparent from the results from the Poincaré sections. The sequence of intersection points reaches an accumulation point after ~ 50 cycles. From then on, the points only fluctuate minimally about the asymptotic limit, with no long term trend.

L377–380 We thank the reviewer for the careful recalculation. Equation (42) was indeed wrong. The error occurred when the equation was rearranged for better readability and transferred to LaTeX-Code. In the actual calculations for the analysis, the correct equation was used. The correct equation is now provided (eq. 28) as well as a short derivation in appendix C. The equation was solved using Newton's method to obtain the critical point for different parameter values (w,T), and the corresponding Jacobians and eigenvalues thereof.

L384–406 The dependence of the eigenvalues on w and T is shown in figures 3 and 4.

L405–413 The paragraph describing the construction of the Poincaré section is now improved and accompanied by a more detailed explanation in appendix D. In fact, the numerical results are needed for the determination of the limit cycle. The periods of the limit cycle are shown in figure 11.

Minor comments

Comments regarding wording are not specifically addressed, since we rewrote the manuscript considering these suggestions.

L11 See General comments.

L24 We changed the text in this respect. In fact, the exact net effect of liquid clouds is not known yet. However, it is known that the albedo effect is usually dominant, thus liquid clouds usually have a cooling impact on Earth's energy budget. We cite now the latest IPCC report for this qualitative behaviour of warm clouds.

L28 In the revised version, the low temperature regime is now mentioned in the first sentence of the introduction.

L41 We added more text, to make clear that they warm the Earth-Atmosphere system.

L50 Sedimentation is important for large crystals. In this work it plays a vital roll for the described mechanism. In the revised version, this is explained in several parts of the manuscript, e.g. in the first paragraph of section 3.1. In fact, the oscillations can only take place because of sedimentation; otherwise, the system would fast reach an equilibrium state.

L79 In the revised version, ∇_x is defined in the passage after equation 1.

L83 We skip this term since it leads to confusion. We investigate an air parcel, i.e. follow the time evolution of the parcel in a Lagrangian way; sedimentation leads to motion of ice crystals relative to the motion of the air parcel.

L90 Splitting up the velocity into different components allows for separation of the sedimentation term in (new) equation 3 and for changing to the Lagrangian perspective.

L94 and L101 For the microphysical parameterisations, non-integer moments arise from integrating power-law relationships with non-integer exponents, as used for mass-length-relations or representations of terminal velocities.

L113 A reference for the two-moment scheme approach is now provided Seifert and Beheng [2006].

L115 J does not depend on r and is therefore just a factor in the integration w.r.t. r. In the revised version, we left out the sentence because stating that "$\partial J/\partial r = 0$" is sufficient.

L159 The geometric standard deviation of the lognormal distribution is dimensionless, it represents the width of the distribution. This has been clarified in the text.

L158–161 We added a reference for the choice of the settings for solution droplet distribution, motivated by observations.

L208 We use a simple power law for representing the columnar shape of the ice crystals in a simple way. For this purpose we "fit" this power law (coefficients C_i and α_i) to a more sophisticated relationship from the Spichtinger and Gierens [2009] model.

L216 We define $S_i = p_v/p_{si} = \mathrm{RH}_i/100\ \%$. Since $q_v/q_{v,si} \approx p_v/p_{si}$, both definitions are almost the same.

L246 See General comments.

L261 We now adjusted the spaces between the units.

L262 For studying the long-term behaviour of SVCs, we have to assure that constant vertical motion is persistent. Slow vertical upward motions $w < 0.05\,\mathrm{m\,s^{-1}}$ can be maintained for quite a long time; examples are motions along warm fronts in the extra-tropics or Kelvin waves in the tropics, leading to almost constant vertical velocities over long time. We provided references for these situation. However, the temperature and pressure change in such situations is quite small; this provides a justification for the assumption of constant temperature and pressure, whereas temperature and pressure changes are used in the evolution equation of relative humidity over ice.

L270-271 The partial derivative term with $\partial/\partial z$ is a hyperbolic term. See also section 2.2.4, point 3.

L292–294 We rewrote the section and added some more details.

L296 We referenced the wrong equation, it was supposed to be (37), now (19).

L299-300 The term $\mathrm{DEP_{RH}}$ is wrong, it has to be $\mathrm{DEP_q}$, since

$$\left.\frac{\mathrm{d}q_c}{\mathrm{d}t}\right|_{Dep} = \mathrm{DEP_q}. \tag{3}$$

The factor ρ was also wrong. However, we changed notation so the terms are not called NUC, DEP, SED anymore. Also, we got rid of ρ in (new) equation (3) using the continuity equation, to avoid confusion.

L315–318 In the following sections, the abbreviation **F** is used for the right hand side of the system, therefore we decided to already introduce it here.

L337 Yes, we mean that relative humidity increases again. Sedimentation removes ice crystals, which constitute a sink for relative humidity due to growth.

L340 State 1 only occurs if either temperature is "rather high" (i.e. right side of the interval $190 \leq T \leq 230\,\mathrm{K}$) or the vertical motion is slow (i.e. left side of the interval $0 < w \leq 0.05\,\mathrm{m\,s^{-1}}$). For the qualitative overview we stay at these vague statements, in the bifurcation diagram the quantitative values are given.

L392 See General comments. The critical point is a stable focus, i.e. a positive (point) attractor.

L422 The critical point was found by first computing the roots wrt RH_i of (new) equation (28), former equation (42). From that, the values for N_c and q_c were derived analytically using (new) equations (C3) and (C4). See appendix C.

L439–441 In the revised version, we state that the bifurcation point is a function of w and T.

L455 Mean sizes are calculated from the mass-size relationship $L = C_i m^{\alpha_i}$, as provided in appendix B. Here, we use the mean mass, as given by $\overline{m} = q_c/N_c$.

L462–464 More details on the Spichtinger and Gierens [2009] model are now given in the first paragraph of section 3.6.

L487 Here we referred to comparison with the model by Spichtinger and Gierens [2009]. We clarified this in the new text.

L502 and L516 "Theoretical" refers to investigations with our simple "analytical" model.

L537 Crystal sizes in this work are to be interpreted as crystal length.

L610 A more detailed outlook on how minimal models could be useful for cloud parameterisations is given in the conclusions of the revised version.

Figure 7 The median is now indicated by a dotted-dashed line.

Figure 9 The correct unit is m s^{-1}.

Response to Ulrike Wacker (reviewer #2)

Theory of dynamical systems

- We reduced some text about description of SVCs. We added text on the mathematical methods and the conceptual model. We included all indicated references.
- We simplified the system introducing summarising coefficients. The relative humidity is not changed by nucleation, since this constitutes a phase transition from liquid to solid, whereas the gas phase is not changed.

  The behaviour of pure ice clouds is completely different than for mixed-phase or pure liquid clouds, which usually exist in a thermodynamic state close to water

saturation. Ice clouds are usually not in thermodynamic equilibrium since ice nucleation takes place at high supersaturations and diffusional growth/evaporation is quite slow. Therefore, relative humidity is an important control variable, which is more natural for ice clouds than specific humidity. Since the system does not fulfil mass conservation, there is no additional benefit from changing the variable from RH_i to q_v but the formulation of the nucleation rate would be more complicated. Therefore we decided not to transform the system into different coordinates.

- We added a paragraph describing the quality of the different terms in the ODE system.
- We expanded the discussion of the mathematical analysis, including figures of eigenvalues etc. .

Terminology We used many terms from theory of dynamical systems from the books by Verhulst [1996] and Argyris et al. [2010]. We tried to change and explain the terms in different ways.

Dry adiabatic lapse rate See general comment.

Derivation of system of equations We have shortened the derivation of equations; especially the description of the cloud processes is now partly transferred to appendix B.

Dimensions We checked all terms again and corrected the inconsistencies.

Minor comments

- We skip the term "Boltzmann equation".
- Equation (9): corrected
- Since the nucleation rate as described by Koop et al. [2000] is formulated as a volume rate, we used this approach. The nucleation rate does not depend on the size of droplets.
- We deleted the term "aerosol particles".
- In contrast to liquid droplet formation the activity is not equal 1 for ice nucleation. The nucleation rate J as described by Koop et al. [2000] can be formulated in terms of differences in water activity (appendix B).
- We changed the layout of equation (16).
- Equation (17) was wrong, now corrected.
- "Length" indicates the length of an ice crystal, i.e. the long side of a columnar-shaped ice crystal.

- Droxtal is the term for very small and almost spherical ice crystals.
- We corrected (former) equation (24)
- We corrected (former) equation (30)
- We use latent heat and heat capacity in molar units, i.e. L_{ice} is actually the molar heat of sublimation; in addition with the molar mass M_{air} and the molar isobaric heat capacity c_p the units in the equations are correct. Please note that we also corrected the equation for adiabatic temperature change.
- We moved the respective text.
- Yes, equation (37) is the correct reference.
- N_a is the number concentration of solution droplets per mass dry air. We skip n_a for clarification.
- We corrected the equation.
- We do not apply $w < 0$ in our model, only upward vertical motions are considered.
- This is correct, the nucleation rate J is positive for $RH_i > 100\%$. Due to the exponential behaviour of J no significant amount of ice crystals is formed at low supersaturations. Only if the supersaturation exceeds certain values (i.e. a "threshold") then a significant amount of ice crystals is produced. We added some text and a reference about the concept of freezing probability and its description by a differential equation, including the nucleation rate.
- We added more text about the use of the Poincaré section for the numerical determination of the limit cycle.
- We rewrote the complete section 3.
- l. 433: Decreased growth rates lead to slower reduction of supersaturation, thus RH_i stays longer above the "freezing thresholds" and more ice crystals can be produced.
- We changed the text from "exponential behaviour" to "power law".
- We restructured section 3.
- We added some more text for describing the features of the models by Spichtinger and Gierens [2009] and Kärcher [2002].
- "Analytical model" refers to the model developed in this study.

- Within the first 4 hours of integrations the oscillation is damped and the amplitude in variables decreases. later, the amplitude of the variables increases again. Admittedly, the system does not reach a "constant" limit cycle, since the properties of the limit cycle are continuously changed by cooling of the temperature. We added some text for clarification.

- We added some text about sources, sinks and forcing terms in the beginning of section 3.

- The microphysical properties of the attractors can be similar, since in the limit cycle case the variables changes within a quite large range that includes also the values of the point attractor.

- We arrange the figure captions in a way that they might be understandable without reading the whole text. Thus, some repetition might be possible.

- The dependence of the mean mass on w is only marginal. We added some text in the manuscript to clarify this issue.

Response to reviewer #3

Discussion of SVCs We enhanced the discussion of SVCs; in fact, we added comparison with remote sensing observations and report more qualitative results of the simulations.

How realistic are model simulations?

- Both states can develop, if previous heterogeneous nucleation takes place. In fact, the system will just start at a different point in phase space.

- We have not investigated the system in details for variations in vertical velocity. In fact, it seems from numerical simulations that for weak perturbations, the system approaches similar states as in the undisturbed scenarios. Theoretical analysis would be much more difficult, since we have no longer an autonomous system. The investigation of this system, externally forced by time-dependent vertical velocities is beyond the scope of our study and is dedicated to future work.

Specific comments

1. Abstract: We changed the text following reviewer's suggestions.

2. Introduction: We skip the word "usually".

3. Introduction: We added more basic references about heterogeneous nucleation. We also added the suggested references by Immler et al., 2008.

4. Section 2, additional settings: We rewrote section 2, changing also the titles of the subsections.

5. We added some text about the change in $n_c = N_c \cdot \rho$ due to temperature/pressure change.

6. We defined ODE in the text.

7. We rewrote the sentences.

8. We added some description of the attractor states, which occur also in the definitions.

9. We added the processes.

10. We changed the text.

11. Former figure 5 (now figure 7) is now described in more details.

12. We changed the wording.

13. We discussed former figure 6 (now figure 8) in more details. The mean mass is shown in figure 10, thus we do not add another panel to figure 6. We added comparison with remote sensing observations considering the issue of subvisible cirrus (or not).

14. In former figure 6 the stable or unstable point attractor is shown. The lines, both solid and dashed, are valid at the respective critical point of the system. The critical point is well defined for both states, it only has different implications, depending on the nature of the state. For the point attractor regime (solid lines), it is a stable focus and the long-term solution approaches it. For the limit cycle regime (dashed lines), the critical point is approximately at the centre of the periodic orbit and provides a good estimate of the mean (or median) properties of the cloud, in terms of mass and number concentration and relative humidity. So the parallel lines in former figure 6, now figure 8, are valid for the critical point which is either a stable focus (solid lines) or an unstable focus (dashed lines).

15. We tried to keep the same wording.

16. We added some text, see also reply to reviewer #2.

Comments to figures

1. We changed the caption.

2. We changed the caption.

3. We changed the figure.

4. It is not possible to add other units, since we refer to different temperature, and thus density, regimes. However, for figure 9 showing the number concentrations for point attractor and limit cycle we added units per litre.

5. Figure 7 (now figure 9): The solid line represents values at the critical point, regardless of the nature of the critical point. It is well defined for both states, see also comment 14.

6. We added some text and we changed the line for the median in the figure. However, the median in the limit cycle case is close to the value at the critical point in the limit cycle regime, not the point attractor. See also comment 14 and comment to figure 6. Limit cycle and point attractor do not coexist, as the environmental conditions determine which state is present.

References

J. Argyris, G. Faust, M. Haase, and R. Friedrich. *Die Erforschung des Chaos*. Springer, Heidelberg, Germany, 2010.

B. Kärcher. Properties of subvisible cirrus clouds formed by homogeneous freezing. *Atmospheric Chemistry and Physics*, 2(2):161–170, 2002.

T. Koop, B. Luo, A. Tsias, and T. Peter. Water activity as the determinant for homogeneous ice nucleation in aqueous solutions. *Nature*, 406(6796):611–614, 2000.

A. Seifert and K. Beheng. A two-moment cloud microphysics parameterization for mixed-phase clouds. part 1: Model description. *Meteorology and atmospheric physics*, 92(1-2): 45–66, 2006.

P. Spichtinger and K. M. Gierens. Modelling of cirrus clouds–part 1a: Model description and validation. *Atmospheric Chemistry and Physics*, 9(2):685–706, 2009.

F. Verhulst. *Nonlinear differential equations and dynamical systems*. Springer, Heidelberg, Germany, 2 edition, 1996.

Manuscript prepared for Nonlin. Processes Geophys.
with version 2014/07/29 7.12 Copernicus papers of the LaTeX class copernicus.cls.
Date: 23 September 2016

Subvisible cirrus clouds – a dynamical system approach

E. J. Spreitzer[1], M. P. Marschalik[1], and P. Spichtinger[1]

[1]Institute for Atmospheric Physics, Johannes Gutenberg University Mainz, Germany

Correspondence to: Peter Spichtinger (spichtin@uni-mainz.de)

Abstract. Ice clouds, so-called cirrus clouds, occur very frequently in the tropopause region. A special class are subvisible cirrus clouds with an optical depth lower than 0.03. Obviously, the ice crystal number concentration of these clouds is very low. The dominant pathway for the formation of these clouds is not known well. It is often assumed that heterogeneous nucleation ~~at~~ on solid aerosol particles is the preferred mechanism although homogeneous freezing of aqueous solution droplets might be possible, since these clouds occur in the low temperature regime $T < 235\,\mathrm{K}$. For investigating subvisible cirrus clouds as formed by homogeneous freezing we develop a simple ~~analytical~~ parcel cloud model from first principles; the model consists of a three dimensional set of ordinary differential equations, ~~including~~ and includes the relevant processes as ice nucleation, diffusional growth and sedimentation~~, respectively~~. We study the formation and evolution of subvisible cirrus clouds in the low temperature regime as driven by slow vertical updraughts ($0 < w \leq 0.05\,\mathrm{m\,s^{-1}}$). The model is integrated numerically and ~~is investigated using~~ also investigated by means of theory of dynamical systems. We found two qualitatively different states for the long-term behaviour of subvisible cirrus clouds. The first state is a point attractor state with a stable focus, i.e. ~~an attractor case and~~ the solution of the differential equations performs damped oscillations and asymptotically reaches a constant value (equilibrium). The second state is a limit cycle ~~scenario~~in phase space, i.e. the solution approaches asymptotically a state of undamped oscillations. The transition between the states constitutes a Hopf bifurcation and is determined by ~~environmental conditions as~~ two parameters – vertical updraughts and temperature. In both cases, the microphysical properties of the simulated clouds agree reasonably well with simulations using a ~~complex~~ more detailed model, with former analytical studies and with observations of subvisible cirrus. In addition, the model can also be used for explaining complex model simulations close to the bifurcation qualitatively. ~~Finally, the~~ The results indicate that homogeneous nucleation ~~might be~~ is a possible formation pathway for subvisible cirrus

clouds. The results motivate a minimal model for SVCs, which might be used in future work for the development of parameterisations for coarse large scale models, representing structures of clouds.

1 Introduction

Clouds consisting exclusively of ice crystals, so-called cirrus clouds, are frequently found in the tropopause region ~~in the extratropics~~at low temperatures ($T < 235\,\mathrm{K}$). Satellite observations show frequencies of occurrence up to 40% in ~~the extratropical~~ extra tropical storm tracks and ~~upto~~ up to 60% in regions of tropical convection (Stubenrauch et al., 2010). Cirrus clouds influence the energy budget of the Earth-Atmosphere system like other clouds by reflecting and scattering incoming solar radiation (albedo effect) and by absorbing and re-emitting thermal radiation (greenhouse effect). ~~In contrast to liquid cloudsthe net effect of cirrus clouds on the total energy budget is not known yet, although usually a positive net effect is~~ For liquid clouds, the albedo effect usually dominates (Stocker et al., 2013, chapter 7) but for pure ice clouds both effects (albedo vs. greenhouse effect) are of comparable absolute size. Therefore microphysical properties (e.g. size or shape, see Zhang et al., 1999) or macrophysical properties (e.g. optical depth or spatial inhomogeneity) can influence the balance between both radiative effects, leading to a net warming or cooling. Nevertheless, for cirrus clouds a net warming of the Earth-Atmosphere system is often assumed (Chen et al., 2000). Since the formation of ice crystals requires high supersaturation ~~(e.g., Koop et al., 2000; Hoose and Möhler, 2012)~~ (see, e.g., Koop et al., 2000; Hoo diffusional growth of ice crystals is quite slow in the low temperature regime (~~$T < 235\,\mathrm{K}$~~$T < 235\,\mathrm{K}$) cirrus clouds ~~usually are~~ mostly exist in a thermodynamic state far away from ~~thermodynamic~~ equilibrium. Thus, in contrast to liquid clouds, which ~~usually~~ approximately coincide with their (super-)saturated environment, for ice clouds there can be a continuous transition from clear air over very low ice crystal number concentrations to thick cirrus clouds with high mass and number concentrations. ~~A special class of cirrus clouds constitute the~~ Cirrus clouds with optical thickness $\tau < 0.03$ constitute a special class, so-called subvisible cirrus clouds (SVCs) ~~, which are usually defined by an optical thickness $\tau < 0.03$~~ (Sassen and Dodd, 1989). These clouds are difficult to ~~detect; usually~~ measure; remote sensing techniques as LIDAR (e.g., Immler et al., 2008b) or occultation observations (e.g., Wang et al., 1996) are used to detect these very thin cirrus clouds. Only few in situ measurements of subvisible cirrus clouds are available, suggesting very low values in ice crystal number concentrations ~~(e.g., Froyd et al., 2010; Kübbeler et al., 2011)~~ (Froyd et al., 2010; Kübbeler et al., 2011) . Global observations from satellites (Wang et al., 1996; Stubenrauch et al., 2010; Hoareau et al., 2013) as well as observations with stationary LIDAR systems ~~(e.g., Sassen and Campbell, 2001; Hoareau et al., 2013)~~ (Sassen and Campbe frequencies of occurrence of about 10–20% in the ~~extratropics~~extra-tropics; in the tropics the frequency of occurrence is much higher (up to 50%, see e.g. Wang et al., 1996). For ~~these~~ subvisible clouds, a net warming of the Earth-Atmosphere system is almost certain, since the albedo effect is almost negligible. Our knowledge ~~about~~ of subvisible cirrus clouds is quite limited. Since the ice crys-

tal number concentration in SVCs is very low, the question about the dominant formation mechanism is still pending. ~~In the cold temperature regime~~ At cold temperatures ($T < 235\,\mathrm{K}$), where pure ice clouds occur, two different formation mechanisms are generally possible, namely heterogeneous nucleation at solid aerosol particles ~~(Hoose and Möhler, 2012)~~ (e.g. Dufour, 1861; aufm Kampe and Weickmann, 1951; Hosler, 1951) homogeneous freezing of aqueous solution droplets ~~(Koop et al., 2000)~~ (Sassen and Dodd, 1989; Koop et al., 2000) . For subvisible cirrus~~Kärcher and Solomon (1999) claimed~~ , Kärcher and Solomon (1999) stated that both nucleation mechanisms might be possible; in contrast, Jensen et al. (2001) and Froyd et al. (2010) clearly suggested that the dominant mechanism ~~should~~ must be heterogeneous nucleation. However, analytical investigations by Kärcher (2002) indicated that also pure homogeneous nucleation might be possible~~, although in this study sedimentation of ice crystals was not explicitly included in the model~~.

In the present study we focus on the formation of SVCs by homogeneous freezing of aqueous solution droplets (~~short~~hereafter: homogeneous nucleation). We study the formation and evolution of SVCs in an air parcel ~~, which~~ that is lifted in slow vertical upward motions (~~$w \leq 0.05\,\mathrm{m\,s^{-1}}$~~$0 < w \leq 0.05\,\mathrm{m\,s^{-1}}$), as typical for synoptic scale motions in the ~~extratropics~~ extra-tropics (e.g. along warm fronts, see Kemppi and Sinclair, 2011) or in slow ascent regions in the tropics, as e.g. driven by Kelvin waves ~~(?) . We include the relevant processes for ice microphysics, i.e. ice nucleation, ice crystal growth due to diffusion of water vapour and sedimentation of ice crystals, respectively~~(Immler et al., 2008a) . We concentrate on the cold temperature regime ($T < 235\,\mathrm{K}$); thus, we exclude the possibility of liquid origin ice clouds (Krämer et al., 2016; Wernli et al., 2016) . This is not a strong limitation since the microphysical properties of ice clouds stemming from mixed phase clouds are quite different, with high ice crystal number and mass concentrations and higher optical depths (Luebke et al., 2016) .

For the investigation of subvisible cirrus clouds we develop a parcel model and to which we apply numerical and analytical tools. The model is developed on the basis of an evolution equation for mass distributions of ice crystals, including a description of microphysical processes based on former work (Spichtinger and Gierens, 2009). ~~However, for using the powerful theory of dynamical systems for analysing the model~~We take into account the relevant processes for ice microphysics, i.e. ice nucleation, ice crystal growth due to diffusion of water vapour, and sedimentation of ice crystals. For applying analytical tools, we make use of some appropriate simplifications in order to obtain an autonomous system of ordinary differential equations (ODEs); the variables of the ~~systems~~ system are ice crystal mass and number concentration, respectively, as well as relative humidity with respect to ice. Thus, we have to investigate a three-dimensional autonomous system of ODEs.

~~In section 2 we describe the development of the model, as derived from a more general approach for mass distributions~~To study the qualitative behaviour of the model we use concepts from theory of dynamical systems (see, e.g., Verhulst, 1996; Argyris et al., 2010) . For autonomous systems of ODEs, equilibrium states can be found easily. The qualitative properties of the system near the

critical points are relevant for the overall behaviour of the system. The stability of these equilibrium states (i.e. point attractors) can be investigated by applying perturbations to the equilibrium states. In fact, we linearise the system at equilibrium points and apply perturbations to this state. The eigenvalues of the linearised system are used for the characterisation of the quality and stability of the equilibrium states. Some theorems are available in order to transfer the qualitative behaviour of the linearised systems to the full nonlinear system. For the characterisation of more complex attractors, as e.g. limit cycles, more sophisticated approaches must be used. For instance, limit cycles can be determined using Poincaré sections (Argyris et al., 2010) . Investigations of cloud models as dynamical systems were carried out for liquid and mixed-phase clouds (Hauf, 1993; Wacker, 1992, 1995, 2006) as well as for cloud-aerosol-precipitation systems (Koren and Feingold, 2011; Feingold and Koren, 2013) . For pure ice clouds such investigations have not been carried out yet. In contrast to clouds involving liquid phase, which are close to thermodynamic equilibrium, we have to consider relative humidity as a control variable, which adds another equation to the system and makes the analysis more challenging. The mathematical characterisation of the model allows for a better understanding of the interaction of different nonlinear processes and the impact of external forcings as vertical updraughts. Finally, the qualitative analysis could be used in future work as starting point for developing cloud parameterisations that represent the qualitative structure of subvisible cirrus clouds.

In section 2 we describe the development of the model. The results of the numerical integration ~~as well as~~ and the mathematical analysis are presented in section 3~~. Here, we also present comparisons with more complex modelsand observations. Finally, we~~ , as well as comparisons with observations and more detailed models. In the final section, we summarise the results, draw some conclusions and give an outlook to future work.

2 Model

In this section we describe the development of a simple model, which is used for analytical and numerical investigations. We include the relevant processes for ~~ice clouds~~ formation and evolution of ice clouds into the model but we try to avoid too much complexity, which makes analysis too complicated (i.e. reducing the complexity paradox, see, e.g., Oreskes et al., 1994; Oreskes, 2003) . Since we investigate subvisible cirrus clouds in the temperature regime $T < 235\,\mathrm{K}$ ~~, namely~~ and at low vertical updraughts $0 < w \leq 0.05\ \mathrm{m\,s^{-1}}$, the relevant processes are ice nucleation, diffusional growth and sedimentation, respectively.

~~We start with the description of~~

2.1 Basic equations

An ice cloud is represented by an ensemble of ice particles~~forming a cloud; for this purpose we use~~ , which can be described by a mass distribution $f(m, \boldsymbol{x}, t)$ with mass of particles, m, as internal coor-

dinate and space, $\boldsymbol{x}$, and time, t, as external coordinates. ~~(Notation follows the convention in population dynamics, see e.g. Ramkrish~~ ~~The procedure is similar to the derivation by Seifert and Beheng (2006) and Beheng (2010)~~ Notation follows the convention in population dynamics (see e.g. Ramkrishna, 2000) . We investigate a test volume with a certain fixed mass of dry air, therefore f has units ~~$[f] = \mathrm{kg}^{-1}$. Thus, we can formulate the evolution equation for f in a Boltzmann-type way~~ $[f] = \mathrm{kg}^{-2}$. The evolution of this mass distribution in time and space is determined by a partial differential equation (see, e.g., Hulburt and Katz, 1964; Seifert and Beheng, 2006; Behen

$$\frac{\partial(\rho f)}{\partial t} + \nabla_x \cdot (\rho \boldsymbol{u} f) + \frac{\partial(\rho g f)}{\partial m} = \rho h. \tag{1}$$

Here, ρ denotes density of air, $\boldsymbol{u}$ and g are the advection velocities in physical space and phase space of the internal coordinate, and h represents sources and sinks for particles. The divergence in physical space is denoted by $\nabla_x = (\partial/\partial x, \partial/\partial y, \partial/\partial z)$. Note, that all functions, $\boldsymbol{u}$, g, h, generally depend on the full set of variables $(m, \boldsymbol{x}, t)$.

~~For the motion of the inertial system we assume a~~ The fluid velocity $\boldsymbol{v} = \boldsymbol{v}(\boldsymbol{x}, t)$ ~~, which is determined by the underlying hydrodynamic motion , governed by some versions or approximations of Navier-Stokes equation. In addition, a single cloud particle might experience a diffusion~~ describes the motion of the air; cloud particles may experience a velocity $\boldsymbol{v}' = \boldsymbol{v}'(m, \boldsymbol{x}, t)$ relative to $\boldsymbol{v}$. ~~The total velocity~~ , thus the total $\boldsymbol{u}$ is ~~thus given by~~

$$\boldsymbol{u}(m, \boldsymbol{x}, t) = \boldsymbol{v}(\boldsymbol{x}, t) + \boldsymbol{v}'(m, \boldsymbol{x}, t).$$

~~Thus, we can reformulate equation as follows:~~

$$\frac{\partial(\rho f)}{\partial t} + \nabla_x \cdot (\rho \boldsymbol{v} f) + \nabla_x \cdot (\rho \boldsymbol{v}' f) + \frac{\partial(\rho g f)}{\partial m} = \rho h.$$

given by $\boldsymbol{u}(m, \boldsymbol{x}, t) = \boldsymbol{v}(\boldsymbol{x}, t) + \boldsymbol{v}'(m, \boldsymbol{x}, t)$. In our study, the only relevant relative velocity of cloud particles is gravitational settling (hereafter: sedimentation), given by a terminal velocity due to balance between gravitational force and drag. The terminal velocity depends on ice crystal mass, i.e. $\boldsymbol{v}' = (0, 0, -v_t(m))$. Note the direction towards Earth's surface, indicated by the minus sign.

~~We have to state here that (even with this simplification)we will not be able to derive a general solution for $f(m, \boldsymbol{x}, t)$. However, since we are interested in bulk quantities as number and mass concentrations, we use the definition of~~ Instead of solving equation (1) for the entire mass distribution, we derive equations for the general moments of $f(m, \boldsymbol{x}, t)$~~:~~ , defined as

$$\mu_k[m](\boldsymbol{x}, t) := \int_0^\infty f(m, \boldsymbol{x}, t)\, m^k \,\mathrm{d}m, \qquad k \in \mathbb{R}. \tag{2}$$

A bounded mass distribution is uniquely determined by all its integer moments (see e.g. Feller, 1971). ~~For deriving equations for the evolution of moments,~~ However, since we cannot (and do not want to) treat an infinite number of moment equations, we ~~multiply equation by m^k and integrate by~~

parts, using $f(0,\boldsymbol{x},t)=0$ and $f(m,\boldsymbol{x},t)\to 0$ for $m\to\infty$, which are physically reasonable assumptions. Thus, we end with the following equation:

$$\frac{\partial(\rho\mu_k)}{\partial t}+\nabla_x\cdot(\rho\boldsymbol{v}\mu_k)+\nabla_x\cdot\left(\int_0^\infty m^k\rho\boldsymbol{v}' f\,\mathrm{d}m\right)=$$

$$k\int_0^\infty m^{k-1}\rho g f\,\mathrm{d}m+\int_0^\infty m^k\rho h\,\mathrm{d}m,\qquad k\in\mathbb{R}.$$

The moments are not restricted to $k\in\mathbb{N}$, instead we allow generalized moments with $k\in\mathbb{R}_{\geq 0}$. Formally, the unit of the k-th moment is $\mathrm{kg}^k\mathrm{kg}^{-1}$.

Since we are interested in processes on cloud scale, we can neglect horizontal diffusion velocities; the remaining relative components of $\boldsymbol{v}'$ are determined by sedimentation of particles, i.e. $\boldsymbol{v}'=(v_1',v_2',v_3')=(0,0,v_3')$ and $v_3'=v_3'(m,\boldsymbol{x},t)$. For simplicity, we assume that the gravitational acceleration of ice particles is very quickly balanced by friction of air, thus we can assume that v_3' is represented by the terminal velocity of an ice particle with mass m, i.e. $v_3'=v_t(m)$. We can include this simplification in the following way:

$$\underbrace{\frac{\partial(\rho\mu_k)}{\partial t}+\nabla_x\cdot(\rho\boldsymbol{v}\mu_k)}_{\text{time evolution + advection}}=\underbrace{-\frac{\partial}{\partial z}\left(\int_0^\infty m^k\rho v_t f\,\mathrm{d}m\right)}_{\text{sedimentation}}$$

$$\underbrace{+k\int_0^\infty m^{k-1}\rho g f\,\mathrm{d}m}_{\text{growth/evaporation}}\quad\underbrace{+\int_0^\infty m^k\rho h\,\mathrm{d}m}_{\text{particle formation/elimination}}.$$

We make the usual ansatz (see e.g. Seifert and Beheng, 2006) for a double moment scheme ($k=0,1$), i.e. $k=0,1$ leading to two prognostic we derive two equations for number concentration ($N_c=\mu_0$) and mass concentration ($q_c=\mu_1$):

$$\frac{\partial(\rho\mu_0)}{\partial t}+\nabla_x\cdot(\rho\boldsymbol{v}\mu_0)$$

$$=\underbrace{-\frac{\partial}{\partial z}\left(\int_0^\infty\rho v_t f\,\mathrm{d}m)\right)}_{SED_n}+\underbrace{\int_0^\infty\rho h\,\mathrm{d}m}_{NUC_n},$$

$$\frac{\partial(\rho\mu_1)}{\partial t}+\nabla_x\cdot(\rho\boldsymbol{v}\mu_1)=$$

$$\underbrace{-\frac{\partial}{\partial z}\left(\int_0^\infty m\rho v_t f\,\mathrm{d}m)\right)}_{SED_q}+\underbrace{\int_0^\infty\rho g f\,\mathrm{d}m}_{DEP_q}+\underbrace{\int_0^\infty m\rho h\,\mathrm{d}m}_{NUC_q}.$$

) of ice crystals from equation (1), of the following form:

$$\underbrace{\frac{\partial \mu_k}{\partial t} + \boldsymbol{v} \cdot \nabla_x \mu_k}_{\text{time evolution + advection}} = \underbrace{\frac{1}{\rho} \frac{\partial}{\partial z} \left(\int_0^\infty m^k \rho v_t f \, \mathrm{d}m \right)}_{\text{sedimentation}} \underbrace{+ k \int_0^\infty m^{k-1} g f \, \mathrm{d}m}_{\text{growth/evaporation}} \underbrace{+ \int_0^\infty m^k h \, \mathrm{d}m}_{\text{particle formation/elimination}}. \tag{3}$$

Here, we also used mass conservation of dry air in order to rewrite the first two terms of equation (1), for details see appendix A. Note the units of N_c and q_c relative to the mass of dry air ~~($[N_c] = \mathrm{kg}^{-1}$, $[q_c] = \mathrm{kg kg}^{-1}$).~~

~~Now we will address the different terms in equations in more details. First, we have to specify the mass concentration in order to close~~ are $[N_c] = \mathrm{kg}^{-1}$ and $[q_c] = \mathrm{kg\,kg}^{-1}$, respectively. For closing the system of ~~two moment equations mathematically.~~

2.2 ~~Choice of distribution~~

~~We~~ equations mathematically, we prescribe a fixed type of mass distribution for the ice crystals~~, namely a lognormal-distribution~~. As in the study by Spichtinger and Gierens (2009) , we use a log-normal-distribution of the following form~~is considered~~:

$$f(m,t) = \frac{N_c(t)}{\sqrt{2\pi} \log \sigma_m} \exp\left(-\frac{1}{2} \left(\frac{\log(\frac{m}{m_m})}{\log \sigma_m} \right)^2 \right) \frac{1}{m}, \tag{4}$$

with ~~the~~ geometric mean mass m_m and ~~the~~ non-dimensional geometric standard deviation σ_m, determining the width of the distribution; log denotes the natural logarithm. The general moments can be described by

$$\mu_k[m] = N_c m_m^k \exp\left(\frac{1}{2} (k \, \log \sigma_m)^2 \right) = N_c \overline{m}^k r_0^{\frac{k(k-1)}{2}}, \tag{5}$$

using the mean mass $\overline{m} = q_c / N_c = \mu_1 / \mu_0$.

~~For this special distributionthe k-th moment is given by~~

$$\mu_k[m] = N_c m_m^k \exp\left(\tfrac{1}{2} (k \log \sigma_m)^2 \right)$$

$$= N_c \bar{m}^k r_0^{\frac{k(k-1)}{2}} = N_c^{-k} q_c^k r_0^{\frac{k(k-1)}{2}}.$$

Here, we ~~use the definition of~~ introduced the dimensionless parameter,

$$r_0 = \frac{\mu_2 \mu_0}{\mu_1^2} = \exp\left((\log(\sigma_m))^2 \right), \tag{6}$$

for closing the set of equations~~. This parameter can also be formulated in terms of the "predominant mass" $m_{pre} = \mu_2 / \mu_1$ (Spichtinger and Gierens, 2009; Höller, 1986) . In the following~~ ; r_0 is set to a constant, thus the geometric standard deviation representing the distribution's width is assumed to be constant. ~~Among others~~ Spichtinger and Gierens (2009) suggest a value of $r_0 = 3$, corresponding to a geometric standard deviation $\sigma_m \approx 2.85$.

2.2 ~~Nucleation~~Parameterisation of relevant processes

In the following the representation of relevant processes is described briefly. For more details we refer to appendix B. Furthermore, we describe additional assumptions for simplification and present the final equations of the model.

2.2.1 Nucleation

For the formation of ice crystals we exclusively consider homogeneous freezing of aqueous solution droplets ~~(e.g. Koop, 2004) . Supercooled solution droplets freeze spontaneously with a nucleation rate J. Similar as for ice particles we can~~ (short: homogeneous nucleation, Koop, 2004) . We describe the ensemble of solution droplets by a size distribution $f_a = f_a(r)$, where r denotes the radius. ~~Again, we set $[f_a] = \mathrm{kg}^{-1}$~~ Units are $[f_a] = \mathrm{kg}^{-1}\mathrm{m}^{-1}$ and f_a is normalised by the total number concentration of ~~aerosol particles~~solution droplets in dry air, $N_a = \mu_0[r]$.

We model homogeneous ~~freezing~~ nucleation as a stochastic process with a nucleation rate J ~~.~~ (for details see appendix B). For the change in the size distribution $f_a(r)$ we can formulate the following equation (acc. to Seifert and Beheng, 2006) ~~Assuming~~ assuming J as a volume rate (i.e. $[J] = \mathrm{m}^{-3}\mathrm{s}^{-1}$):

$$\left.\frac{\partial(\rho f_a(r))}{\partial t}\frac{\partial f_a(r)}{\partial t}\right|_{\text{freezing}\,\text{nucleation}} = -\frac{4}{3}\pi r^3 J \rho f_a(r). \tag{7}$$

Integration of the equation leads to an equation for the total loss of ~~aerosol particles~~ solution droplets

$$\frac{\partial(\rho N_a)}{\partial t}\frac{\partial N_a}{\partial t} = -\frac{4}{3}\pi\rho\int_0^\infty r^3 J f_a(r)\,\mathrm{d}r. \tag{8}$$

~~assuming~~ Assuming a bijective relation between ice crystals and ~~aerosol particles~~solution droplets, we combine the total gain of ice particles as ~~:~~

$$\frac{\partial(\rho N_c)}{\partial t}\frac{\partial N_c}{\partial t} = -\frac{\partial(\rho N_a)}{\partial t}\frac{\partial N_a}{\partial t} = \frac{4}{3}\pi\rho\int_0^\infty r^3 J f_a(r)\,\mathrm{d}r = \frac{4}{3}\pi\rho J\mu_{3,a}[r], \tag{9}$$

where ~~$t_{3,a}$~~ $\mu_{3,a}[r]$ denotes the third moment of the size distribution of solution droplets. Here, we assume that $\partial J/\partial r = 0$~~, thus we can treat the integral as a constant.~~

~~Since~~ . Since the ice crystal number concentration in SVCs is very low, we assume that only a minor fraction of solution droplets is converted to ice ~~, we can assume that~~ and the size distribution ~~will be~~ remains constant in time. Thus, the third moment can be calculated once and is then used as a constant ~~, given by the type and parameters of $f_a(r)$~~in the resulting equations. We assume $f_a(r)$ as a ~~lognormal~~ log-normal distribution with a modal radius of $r_m = 100\,\mathrm{nm}$, a dimensionless geometric standard deviation $\sigma_r = 1.5$ and a total number concentration $\rho N_a = 3\times10^8\,\mathrm{m}^{-3}$~~. Koop et al. (2000) give a parameterisation for the nucleation rate coefficient J as a~~

~~function of $\Delta a_w := a_w - a_w^i$ (Koop et al., 2000, Table 1, eq. 7) . Here a_w is the water activity of the solution and a_w^i is the water activity of the solution in equilibrium with ice. Note, that the freezing characteristics of the droplets do not depend on the chemical composition. By definition the water activity is the ratio e_{sol}/e_{liq} of the vapor pressure over a solution, e_{sol}, and pure liquid water, e_{liq}. Neglecting the Kelvin effect and assuming that the solution droplets are in equilibrium with the environment ($e = e_{sol}$), the water activity is proportional to the water activity in equilibrium with ice, which is the ratio of the water vapour pressure over ice and pure liquid water:~~

$$a_w = \frac{e_{sol}}{e_{liq}} = \frac{e}{e_{liq}} = \frac{RH_i}{100\%}\frac{e_i}{e_{liq}} = \frac{RH_i}{100\%}a_w^i.$$

~~Both e_i and e_{liq}, only depend on temperature and are parameterised according to Murphy and Koop (2005, eq. 7 and 10, respectively) Hence, Δa_w is a function of RH_i and T, as given by~~

$$\begin{aligned}\Delta a_w(T, RH_i) &= \left(\tfrac{RH_i}{100\%} - 1\right) a_w^i(T) \\ &= \left(\tfrac{RH_i}{100\%} - 1\right) \tfrac{e_i}{e_{liq}}.\end{aligned}$$

~~Therefore J is also a function of RH_i and T.~~

~~The logarithm of the nucleation rate is parameterised by a third order polynomial in Δa_w (Koop et al., 2000, table1, eq. 7) :~~

$$\begin{aligned}\log_{10} J(T, RH_i) = &-906.7 + 8502\ \Delta a_w \\ &-26924(\Delta a_w)^2 + 29180(\Delta a_w)^3.\end{aligned}$$

~~With this, we can formulate the two terms for particle generation:~~ , similar to the settings by Spichtinger and Gierens (2009) , which are motivated by observations (Minikin et al., 2003) . This leads to a formulation of

$$NUC_n = \frac{\partial(\rho N_c)}{\partial t}\frac{\partial N_c}{\partial t}\bigg|_{NUC\,\text{nucleation}} = \frac{4}{3}\pi\rho N_a \rho r_m^3 \exp\left(\frac{1}{2}(3\log\sigma_r)^2\right) J(RH\text{RH}_i, T) \tag{10a}$$

and

$$NUC_q \frac{\partial q_c}{\partial t}\bigg|_{\text{nucleation}} = m_0 NUC_n \cdot \frac{\partial N_c}{\partial t}\bigg|_{\text{nucleation}}, \tag{10b}$$

using a typical droplet mean mass $m_0 = 10^{-15}\,\text{kg}$ (size $\sim 1\,\mu\text{m}$) in the spirit of the mean value theorem. The nucleation rate J is parameterised according to Koop et al. (2000) and can be expressed as a function of relative humidity with respect to ice and temperature. For further details see appendix B.

2.3 ~~Depositional growth~~

~~The growth~~

2.2.1 Diffusional growth

The growth and evaporation of ice crystals is dominated by diffusion ~~. The "advection velocity" g in the mass space is given by~~ of water vapour. With several simplifications of the growth equation ~~for a single ice crystal; this equation has the following form (see, e.g., Stephens, 1983) :~~

$$g(m) = \frac{\mathrm{d}m}{\mathrm{d}t} = 4\pi C D_v^* \rho (q_v - q_{v,si}) f_v.$$

~~Here, $q_{v,s} = \varepsilon p_{si}(T)/p$ denotes the saturation mixing ratio, the shape of the ice crystal is accounted for by the capacity C (assuming the electrostatic analogy, see e.g. McDonald, 1963; Jeffreys, 1918) , D_v^* is the full diffusion constant including the kinetic correction for small particles (Lamb and Verlinde, 2011) and f_v denotes the ventilation coefficient.~~

~~In this study we make use of the following simplifications: Latent heat release at the crystal surface is neglected and the temperature of the ice particles is assumed to be equal to temperature of ambient air. We neglect kinetic corrections, since we are mostly interested in growth of larger crystals. Thus, we can assume~~

$$D_v^* \approx D_v = D_0 \left(\frac{T}{T_0}\right)^{\alpha} \left(\frac{p_0}{p}\right),$$

~~with $D_0 = 2.11 \cdot 10^{-5}\,\mathrm{m^2 s^{-1}}$, $T_0 = 273.15\,\mathrm{K}$, $p_0 = 101325\,\mathrm{Pa}$, $\alpha = 1.94$ (e.g. Pruppacher and Klett, 1997) . We neglet correction of ventilation, setting $f_v = 1$. Since ventilation correction is relevant for very large crystals, this is a reasonable assumption. The shape of ice crystals, is assumed to be prolate spheroids with a length and an eccentricity ε', this leads to the following expression (McDonald, 1963) :~~

$$C = L \frac{\varepsilon'}{\log\left(\frac{1+\varepsilon'}{1-\varepsilon'}\right)}.$$

~~For the mass-size relation we assume a simple power law $L(m) = C_i m^{\alpha_i}$ using~~ (for details see appendix B) we obtain the following equation for diffusional growth of a single crystal:

$$g(m) \approx \frac{4}{3}\pi C_i D_v m^{\alpha_i} \rho q_{v,si} (S_i - 1), \tag{11}$$

with constants $C_i = 1.02\,\mathrm{m}$, $\alpha_i = 0.4$ ~~, which was fitted to the more complex description in Spichtinger and Gierens (2009) , where a transition between droxtals and columns is formulated and used.~~

~~The fraction in equation only depends weakly on the crystal mass and can be approximated by a constant mean value of $1/3$. This yields~~

$$C = \frac{1}{3} C_i m^{\alpha_i}.$$

~~Thus, we end with the simplified expression for $g(m)$:~~

$$g(m) \approx \frac{4}{3}\pi C_i m^{\alpha_i} \rho (q_v - q_{v,si})$$

$$= \frac{4}{3}\pi C_i m^{\alpha_i} \rho q_{v,si}(S_i - 1),$$

~~using the~~ and using saturation ratio $S_i = p_v/p_{si}$ and ~~the~~ saturation mixing ratio

$$q_{v,si}(T,p) = \frac{\varepsilon p_{si}(T)}{p}.,$$ (12)

~~Thus, we can derive the term DEP_q in equation~~ respectively. We can express the term for diffusional growth in the moment equations (3) by integration, i.e.:

$$DEP_q \left.\frac{\mathrm{d}q_c}{\mathrm{d}t}\right|_{\text{growth}} = \int_0^\infty \rho g(m) f(m)\,\mathrm{d}m = \frac{4}{3}\pi C_i D_v \rho q_{v,si}(S_i - 1)\mu_{a_i}[m]$$

$$= \frac{4}{3}\pi C_i D_v \rho q_{v,si}(S_i - 1) n N_c^{1-\alpha_i} q_c^{\alpha_i} r_0^{\frac{\alpha_i(\alpha_i-1)}{2}}.$$ (13)

2.3 ~~Sedimentation~~

2.2.1 Sedimentation

~~For the derivation of the terms SED_q, SED_n we use the mean value theorem for describing the relevant integrals in equation as follows:~~

$$\int_0^\infty v_t(m)\rho m^k f(m)\,\mathrm{d}m = \bar{v}_k \int_0^\infty \rho m^k f(m)\,\mathrm{d}m = \rho \bar{v}_k \mu_k.$$

~~Thus, we can~~ Following Spichtinger and Gierens (2009) , we describe the weighted terminal velocity $\bar{v}_k$ for the flux of the k-th moment as

$$\bar{v}_k = \frac{1}{\mu_k}\int_0^\infty v_t(m) m^k f(m)\,\mathrm{d}m.,$$ (14)

(for details see appendix B). Here, we use a simple power law for the representation of the terminal velocity ~~in addition with~~

$$v_t(m) = \gamma m^\delta \mathrm{corr}(T,p)$$ (15)

with $\gamma = 63292.36\,\mathrm{m\,s^{-1}\,kg^{-\delta}}$, $\delta = 0.57$ and a density correction term ~~$c(T,p)$, i.e.:~~

$$v_t(m) = \gamma m^\delta c(T,p)$$

~~where~~

$$c(T,p) = \left(\frac{p}{p_{00}}\right)^{a_i}\left(\frac{T}{T_{00}}\right)^{a_2},$$

~~$T_{00} = 233\,\mathrm{K}$, $p_{00} = 300\,\mathrm{Pa}$, $a_1 = -0.178$, $a_2 = -0.397$ (see e.g. Spichtinger and Gierens, 2009) and $\gamma = 63292.36\,\mathrm{ms}^{-1}\mathrm{kg}^{-\delta}$, $\delta = 0.57$. Thus, we obtain the weighted velocities for number and mass flux, respectively, in the following form:~~

$$\bar{v}_0 = \bar{v}_n = \gamma \tfrac{\mu_\delta}{\mu_0} c(T,p),$$

$$\bar{v}_1 = \bar{v}_q = \gamma \tfrac{\mu_{\delta+1}}{\mu_1} c(T,p).$$

$\mathrm{corr}(T,p)$ (see appendix B).

We can ~~formulate~~ compose the general terms for sedimentation in the moment equations (3):

$$SED_n = \frac{\partial}{\partial z}\left(\rho \bar{v}_n N_c\right) = \frac{\partial}{\partial z}\left(\rho\gamma \cdot \mu_{\delta+1}[m] c_\delta[m] \cdot \mathrm{corr}(T,p)\right), \tag{16a}$$

$$SED_q = \frac{\partial}{\partial z}\left(\rho \bar{v}_q q_c\right) = \frac{\partial}{\partial z}\left(\rho\gamma \cdot \mu_{\delta}[m] c_{\delta+1}[m] \cdot \mathrm{corr}(T,p)\right). \tag{16b}$$

2.3 ~~Additional settings~~

2.2.1 Simplifications

In order to ~~formulate~~ obtain a consistent but simplified system of ordinary differential equations we make the following assumptions:

1. ~~Instead of an Eulerian~~ Change to Lagrangian point of view ~~we change~~ and purely vertical motion:
   Since we are interested in the time evolution of cloud variables in a single air parcel, we change our point of view from Eulerian description to a Lagrangian viewpoint~~, i. e. the~~. The Eulerian time evolution and advection of a quantity ϕ in the fluid motion ~~,~~

   $$\frac{\partial(\rho\phi)}{\partial t} + \nabla_x \cdot (\rho \boldsymbol{v} \phi),$$

   can be seen as total time derivative $\frac{\mathrm{d}(\rho\phi)}{\mathrm{d}t}$

   $$\frac{\mathrm{d}\phi}{\mathrm{d}t} = \frac{\partial \phi}{\partial t} + \boldsymbol{v} \cdot \nabla_x \phi, \tag{17}$$

   representing the Lagrangian description. Note that motions relative to the Lagrangian evolution are still included, i.e. sedimentation still plays a role.

   ~~We will generally focus on the development inside a prescribed parcel, thus the Langrangian description is adequate.~~ We will exclusively consider vertical motions of the air parcel as driven by a vertical velocity component w, i.e. $\boldsymbol{v} = (0,0,w(t))$. ~~Vertical~~ In order to close the system, equations for temperature and pressure must be derived. The vertical motion of the air parcel ~~will lead to adiabatic processes, i.e. compression or expansion, leading to temperature /pressurechanges~~ $\frac{\mathrm{d}T}{\mathrm{d}t}$, $\frac{\mathrm{d}p}{\mathrm{d}t}$ ~~assuming hydrostatic balance , we can explicitly describe the temperature~~

/leads to adiabatic changes in temperature and pressure. Since we can assume hydro-static balance for pressure in a very good approximation, we explicitly describe temperature and pressure rates:

$$\frac{\mathrm{d}T}{\mathrm{d}t} = \frac{\mathrm{d}T}{\mathrm{d}z}\frac{\mathrm{d}z}{\mathrm{d}t} = -\frac{g}{cp}\frac{g \cdot M_{air}}{c_p} w \frac{\mathrm{d}p}{\mathrm{d}t}, \qquad \frac{\mathrm{d}p}{\mathrm{d}t} = \frac{\mathrm{d}p}{\mathrm{d}z}\frac{\mathrm{d}z}{\mathrm{d}t} = -g\rho w. \tag{18}$$

whereas g denotes acceleration of gravity, M_{air} is the molar mass of dry air and c_p is the molar isobaric heat capacity. We would expect additional temperature changes due to phase changes (latent heat release), when ice crystals grow or evaporate by water vapour diffusion. However, since we investigate ice clouds in the low temperature regime, temperature changes due to latent heat release can be neglected in good approximation. For low temperatures ($T < 235\,\mathrm{K}$) the deviation from the dry adiabatic lapse rate is less than 5% and is decreasing with decreasing temperature Therefore, we omit temperature change due to latent heat release, which would appear as an additional nonlinear term in the system of equations.

2. Closure using an equation for relative humidity w.r.t. ice:

   In our study, we will exclusively consider very low vertical velocities ~~or vertical changes with limited amplitude. Thus, we can approximately assume that temperature and pressure are constant. In consequence, we also keep the volume of our air parcel constant and due to the ideal gas law, density remains constant, too. Hence, ρ drops out in equation and all equations derived from it~~($0 < w \leq 0.05\,\mathrm{m\,s^{-1}}$), which are typical for formation of SVCs in large-scale upward motions. Variations in w, i.e. time-dependent velocities $w(t)$ are not investigated since our main focus is to understand the behaviour of SVCs in this quite simple but realistic setup. Time-dependent vertical velocities would largely complicate our investigations and thus is beyond the scope of this study. At low vertical updraughts, temperature and pressure do not change much. At an updraught velocity of ~~$w = 2 \cdot 10^{-2}\mathrm{ms}^{-1}$~~$w = 0.02\,\mathrm{m\,s^{-1}}$, for instance, temperature would decrease by about 0.7 K per hour~~, meaning that after twelve hours the temperature difference~~. If an updraught of this strength were sustained for 12 h, the resulting temperature decrease would be about ~~8 K. However, we are not primarily interested in a highly accurate model, but rather a model that is as simple as possible, describes the aspects of the mechanism qualitatively.~~ 8 K. A persistence of such weak updraughts for a long time is realistic for warm fronts at mid latitudes (Kemppi and Sinclair, 2011) or Kelvin waves in the tropics (Immler et al., 2008a) .

   ~~Finally, we can use this assumption for approximating the sedimentation terms. We have to consider terms of the form~~

   ~~$$\frac{\partial}{\partial z}(\rho \bar{v}_k \mu_k) \qquad k = 0, 1,$$~~

   ~~i.e. vertical changes in the sedimentation flux, $j_k = \rho \bar{v}_k, \mu_k$. Since the volume does not change we assume a box with volume $V = A \cdot \Delta z$ with constant vertical extension Δz and~~ Thus, as

temperature decrease at slow upward motions is only very small, in a zeroth order approximation we assume constant ~~base area A. The sedimentation flux j_k is perpendicular to the surface of the base area. To avoid a hyperbolic term in our equations, we approximate the vertical change of the flux by centered differences:~~

$$\frac{\partial}{\partial z} j_k \approx \frac{1}{\Delta z}\left(j_k^{\text{top}} - j_k^{\text{bottom}}\right)$$

$$= \frac{1}{\Delta z}\left((\rho \bar{v}_k \mu_k)^{\text{top}} - (\rho \bar{v}_k \mu_k)_k^{\text{bottom}}\right).$$

~~We investigate the top layer of a cloud, therefore by definition $j_k^{\text{top}} = 0$. Hence, we can write:~~

$$SED_n \quad = -\frac{\rho \bar{v}_N \mu_0}{\Delta z} = -\rho\gamma \frac{\mu_\delta}{\Delta z} c(T,p)$$

$$SED_q \quad = -\frac{\rho \bar{v}_q \mu_1}{\Delta z} = -\rho\gamma \frac{\mu_{\delta+1}}{\Delta z} c(T,p).$$

temperature and pressure. In consequence, the parcel's volume remains constant, too. The resulting error for neglecting density changes is usually of order $\sim 10\%$ (see e.g. Weigel et al., 2015) .

Since we are ~~mostly interested in the top cloud layer, where ice nucleation occurs (see, e.g., Spichtinger and Gierens, 2009) , we set the thickness of the cloud layer to $\Delta z = 50\,\text{m}$.~~ primarily interested in a simple conceptual model describing the main properties of SVCs, these assumptions are justified.

To close the systems of differential equations we introduce an evolution equation for relative humidity, starting with the total derivative of ~~$RH_i = pq_v/(\varepsilon p_{si}(T))$:~~ $RH_i = 100\% pq_v/(\varepsilon p_{si}(T))$:

$$\frac{\mathrm{d}RH_i}{\mathrm{d}t}\frac{\mathrm{d}RH_i}{\mathrm{d}t} = \frac{\partial RH_i}{\partial T}\frac{\partial RH_i}{\partial T}\frac{\mathrm{d}T}{\mathrm{d}t} + \frac{\partial RH_i}{\partial p}\frac{\partial RH_i}{\partial p}\frac{\mathrm{d}p}{\mathrm{d}t} + \frac{\partial RH_i}{\partial q_v}\frac{\partial RH_i}{\partial q_v}\frac{\mathrm{d}q_v}{\mathrm{d}t}. \tag{19}$$

~~The ascent of the air parcel is purely adiabatic and no diabatic effects are taken into account. Thus~~While temperature and pressure remain approximately the same during parcel ascent, the relative humidity should be affected by terms involving $\mathrm{d}T/\mathrm{d}t$ and $\mathrm{d}p/\mathrm{d}t$, respectively. Neglecting latent heat release as stated above, the first two ~~contributions are given by~~terms in equation (19) read:

$$\frac{\partial RH_i}{\partial T}\frac{\mathrm{d}T}{\mathrm{d}t} = RH_i \frac{M_{air}}{RT^2} L_{ice} \cdot \frac{g}{c_p} w, \tag{20a}$$

$$\frac{\partial RH_i}{\partial p}\frac{\mathrm{d}p}{\mathrm{d}t} = \frac{RH_i}{p} \cdot \rho g w = -RH_i \frac{M_{air}}{RT} g w, \tag{20b}$$

~~making use of equation , the dry adiabatic lapse rate, and the hydrostatic equilibrium.~~ M_{air} is the molar mass of dry air and L_{ice} is the molar heat of sublimation; we use the parameterisation for L_{ice} by Murphy and Koop (2005). As usual, g denotes ~~the~~ gravitational acceleration and c_p is the molar isobaric heat capacity of air. ~~Since these two expressions account for the change of~~

~~RH_i due to adiabatic cooling they are subsumed under $COOL_{RH}$. Note that using assumption~~ ~~??,~~ Note that we only consider temperature ~~/~~and pressure changes in equation (19), but leave temperature and pressure constant otherwise. Therefore, we do not include the equations for $\mathrm{d}T/\mathrm{d}t$ and $\mathrm{d}p/\mathrm{d}t$ in our ODE system of the model. This approach will be useful for analytical investigations~~.~~, although this implies a slight inconsistency. This allows us to study the long term behaviour of the system.

The last term in equation (19) represents the sink due to diffusional growth of ice particles and ~~is denoted as DEP_{RH},~~ can be written as:

$$\frac{\partial RH_i}{\partial q_v}\frac{\mathrm{d}q_v}{\mathrm{d}t} = -\frac{\partial RH_i}{\partial q_v}\frac{\mathrm{d}q_c}{\mathrm{d}t}\bigg|_{\text{growth}} = -\frac{4}{3}\pi\rho D_v C_i (RH_i - 100\%) r_0^{\frac{\alpha_i(\alpha_i-1)}{2}} N_c^{1-\alpha_i} q_c^{\alpha_i}. \tag{21}$$

We use relative humidity as a control variable instead of specific humidity, which has been used in former studies (e.g. Hauf, 1993; Wacker, 1992) for liquid or mixed-phase clouds close to thermodynamic equilibrium (water saturation). Since pure ice clouds commonly exist at states far away from equilibrium, relative humidity (or equivalently saturation ratio) is the relevant thermodynamic variable. In addition, the representation of processes changing this variable or depending on this variable is much easier than for specific humidity q_v, e.g. in the nucleation parameterisation.

3. Approximation of sedimentation

   Since we are interested in an analytically treatable model of a single air parcel, we would like to get rid of partial derivatives describing sedimentation, which generally lead to a hyperbolic system of partial differential equations, which is too complicated for theoretical analysis. For simplification of the equations we have to consider terms of the form

$$\frac{\partial}{\partial z}(\rho \bar{v}_k \mu_k) \qquad k = 0, 1, \tag{22}$$

   i.e. ~~:~~ vertical gradients in the sedimentation flux, $j_k = \rho \bar{v}_k \mu_k$. Since the volume does not change, we assume a box with volume $V = A \cdot \Delta z$ with constant vertical extension Δz and constant base area A. The sedimentation flux j_k is perpendicular to the surface of the base area. We approximate the vertical change of the flux by centred differences:

$$\frac{\partial}{\partial z} j_k \approx \frac{1}{\Delta z}\left(j_k^{\text{top}} - j_k^{\text{bottom}}\right) = \frac{1}{\Delta z}\left((\rho \bar{v}_k \mu_k)^{\text{top}} - (\rho \bar{v}_k \mu_k)_k^{\text{bottom}}\right). \tag{23}$$

We investigate the top layer of a cloud, therefore by definition $j_k^{\text{top}} = 0$. Hence, we can write:

$$DEP_{RH} = \frac{\partial RH_i}{\partial q_v}\frac{\mathrm{d}q_v}{\mathrm{d}t} = \frac{1}{\rho}\frac{\partial}{\partial z}(\rho \bar{v}_N \mu_0) \approx -\frac{\partial RH_i}{\partial q_v}\frac{\mathrm{d}q_c}{\mathrm{d}t}\frac{\bar{v}_N \mu_0}{\Delta z} = -\frac{\partial RH_i}{\partial q_v} \cdot \frac{1}{\rho} DEP_{RH} \gamma \frac{\mu_\delta}{\Delta z} c(T,p), \tag{24a}$$

$$\frac{1}{\rho}\frac{\partial}{\partial z}(\rho \bar{v}_q \mu_1) \approx -\frac{\bar{v}_q \mu_1}{\Delta z} = -\frac{4}{3}\pi \rho D_v C_i \gamma \frac{\mu_{\delta+1}}{\Delta z} c(RH_i - 100\%T, p) r_0^{\frac{\alpha_i(\alpha_i-1)}{2}} N_c^{1-\alpha_i} q_c^{\alpha_i}. \tag{24b}$$

2.3 ~~System of ODEs~~

2.2.1 Final system of ODEs

In summary, the full system of the model equations reads:

$$\frac{\mathrm{d}N_c}{\mathrm{d}t} = \frac{4\pi}{3}\frac{n_a}{\rho} r_m^3 \exp\left(\frac{1}{2}(3\ln(\sigma_r))^2\right) J(RH_i, T) - \frac{\gamma\, c(T,p)}{\Delta z} r_0^{\frac{\delta(\delta-1)}{2}} N_c^{1-\delta} q_c^{\delta}$$

$$\frac{\mathrm{d}q_c}{\mathrm{d}t} = m_0 \frac{4\pi}{3}\frac{n_a}{\rho} r_m^3 \exp\left(\frac{1}{2}(3\ln(\sigma_r))^2\right) \cdot J(RH_i, T) - \frac{\gamma\, c(T,p)}{\Delta z} r_0^{\frac{\delta(\delta+1)}{2}} N_c^{-\delta} q_c^{1+\delta} + \pi\varepsilon\rho D_v C_i \frac{e_i}{p}\left(\frac{RH_i}{100\%} - 1\right) r_0^{\frac{\alpha_i(\alpha_i-1)}{2}} N_c^{1-\alpha_i} q_c^{\alpha_i}$$

$$\frac{\mathrm{d}RH_i}{\mathrm{d}t} = RH_i g w \frac{M_{air}}{RT}\left(\frac{L_{ice}}{c_p T} - 1\right) - \pi\rho D_v C_i (RH_i - 100\%) r_0^{\frac{\alpha_i(\alpha_i-1)}{2}} N_c^{1-\alpha_i} q_c^{\alpha_i}.$$

$$\frac{\mathrm{d}N_c}{\mathrm{d}t} = \underbrace{a \cdot J(RH_i, T)}_{\text{nucleation}} \underbrace{-b \cdot N_c^{1-\delta} q_c^{\delta}}_{\text{sedimentation}} \tag{25a}$$

$$\frac{\mathrm{d}q_c}{\mathrm{d}t} = \underbrace{a \cdot m_0 \cdot J(RH_i, T)}_{\text{nucleation}} \underbrace{-c \cdot N_c^{-\delta} q_c^{\delta-1}}_{\text{sedimentation}} \underbrace{+ d \cdot (RH_i - 100\%) N_c^{1-\alpha_i} q_c^{\alpha_i}}_{\text{growth}} \tag{25b}$$

$$\frac{\mathrm{d}RH_i}{\mathrm{d}t} = \underbrace{e \cdot w \cdot RH_i}_{\text{vertical motion}} \underbrace{-f \cdot (RH_i - 100\%) N_c^{1-\alpha_i} q_c^{\alpha_i}}_{\text{growth}} \tag{25c}$$

where $a, b, c, d, e, f > 0$ denote positive real constants as indicated in appendix B. Note that almost all coefficients also depend on the (fixed) parameter T. This is an autonomous system of ordinary

differential equations~~. For better readability the equations are abbreviated:~~ , i.e. we can write the system in the following form:

$$\dot{\boldsymbol{x}} = \boldsymbol{F}(\boldsymbol{x}), \qquad \text{with } \boldsymbol{x} = (N_c, q_c, ~~RH_i~~ RH_i)^T, \tag{26}$$

and $\boldsymbol{F}$ the right hand side of (25). Note that the assumption of constant temperature, pressure and vertical velocity ensures that the system (25) possesses critical points.

3 ~~Results~~

2.1 ~~General features~~Setup

We examine the system for a range of parameter values ~~$0 < w \leq 0.05\,\mathrm{m\,s^{-1}}$ and~~ $0 < w \leq 0.05$ m s^{-1} and ~~$190\,\mathrm{K} \leq T \leq 230\,\mathrm{K}$~~$190\,\mathrm{K} \leq T \leq 230$ K, at a ~~pressure of $p = 300\,\mathrm{hPa}$~~constant pressure of $p = 300$ hPa, which corresponds to upper tropospheric conditions with moderate vertical motions as in synoptic weather situations or slow upward motions in the tropics (e.g. Kelvin waves). ~~The~~

We investigate the model using analytical tools (see details in section 3) and also integrate the model numerically. For this purpose, the air parcel is ~~initialized~~ initialised with no ice particles ($N_c(0) = 0$, $q_c(0) = 0$) and at high supersaturation w.r.t. ice (~~$RH_i(0) = 140\,\%$~~$RH_i(0) = 140$ %). The prognostic equations (25) are integrated numerically ~~using~~ with the *LSODA* algorithm from the ~~Fortran~~ FORTRAN library *ODEPACK* (Hindmarsh, 1983).

3 Results

3.1 General features of the system

The general cloud formation mechanism works as follows: The adiabatic cooling causes the relative humidity, and thus the nucleation rate, to rise until ~~the freezing probability is high enough to allow ice nucleation . This corresponds merely with~~ ice nucleation occurs. Due to the steepness of J with respect to RH_i, occurrence of ice nucleation corresponds approximately to a threshold in relative humidity ~~. According to Ren and Mackenzie (2005) , this threshold might be expressed as $RH_{i,crit} = (2.349 - T/259) \cdot 100\%$, i.e. $RH_{i,crit} \approx 140$–150%~~($\sim 140 - 150$ %, see, e.g., Ren and Mackenzie, 2005; Kärcher and L
The stronger the dynamical forcing w, the stronger the nucleation event and the more ice particles form. Ice particle growth then reduces the relative humidity ~~and hence the freezing rate is also reduced~~ (see equation (19), last term) ~~. The crystals, that have become large, fall out , thus sedimentation reduces the ice crystal concentrations, which causes relative humidity to further increase . In fact, sedimentation is the key process , which leads to different states in the cloud evolution. The~~ and hence the nucleation rate is also reduced. Crystals grow to larger sizes and begin to sediment out of the air parcel. Sedimentation reduces ice crystal mass and number concentrations, and thus weakens the growth term. Then relative humidity can increase again allowing the cycle to start over.

The sedimentation process allows for oscillations in the system; without sedimentation (the only sink for N_c and q_c) a steady state at ice saturation would be reached soon (see e.g. Kärcher, 2002; Spichtinger and Gierens, 2009) .

From the numerical simulations we found that the system exhibits two qualitatively distinct behaviours, depending on ~~the parameter~~ values of w and T.

~~State 1:~~ First, we give a qualitative overview:

State 1: At rather high temperatures and slow vertical velocities, the three competing microphysical processes (nucleation, growth, sedimentation) are relatively slow and act on similar time scales, so none of them is dominant. In particular, ~~freezing~~ nucleation rates are rather small in these cases, therefore only few ice crystals are formed initially, which grow and also sediment quite slowly. The three processes are more or less in balance, resulting in a damped oscillation in all three variables, ~~finally~~ N_c, q_c, RH_i, asymptotically reaching an equilibrium state~~in numerical integrations of equations~~ , as shown in figure 1. Note, that in this state, nucleation is ~~occurring continuously, as relative humidity remains above the freezing threshold~~ always present, as strong supersaturation with relative humidity close to the nucleation threshold persists at all times and thus the nucleation rates are high enough to produce ~~ice crystals~~considerable amounts of ice crystals continuously. This results in smooth oscillations instead of sharp nucleation events, as usually expected (see, e.g., Kärcher and Lohmann, 2002) . If the air parcel is not disturbed and the vertical updraught remains unchanged in the long term evolution, the cloud ~~that forms will persist and will have~~ persists and has constant microphysical properties. The cloud in the steady state typically contains low crystal concentrations. The dynamic equilibrium remains at high supersaturations, i.e. ~~is far~~ the cloud stays far away from thermodynamic equilibrium. ~~The cloud properties are discussed quantitatively in section ?? in more detail.~~

~~State 2:~~

State 2: When increasing w or decreasing T, respectively, to a certain level, ~~there is no damping and stationarity is not reached~~ oscillations in variables N_c, q_c, RH_i are not damped anymore (see figure 2) ~~because the processes are not in balance in this case~~and no asymptotic equilibrium can be observed (as e.g. a point in phase space). Instead, we obtain pulse-like nucleation with distinct nucleation events ~~and the nucleation rates fall far below the critical rates at $RH_{i,crit}$~~followed by phases with almost vanishing nucleation rates at low relative humidities. The amplitude of the oscillation is very large in all variables~~and the~~ ; due to sedimentation ice particle concentration is reduced to a small fraction of the maximum value once in a period. At colder temperatures and faster vertical velocities, the nucleation rates are much higher, so ~~freezing~~ nucleation is the dominant process in the beginning, leading to pulse nucleation events. After a while, ice crystal growth becomes dominant and when the crystals have become

large, sedimentation sets in and crystal numbers decrease rapidly. Finally, the cycle starts over. In this case, the ~~freezing~~ nucleation events are clearly separated, as opposed to the first case. ~~In~~ For the time evolution we find that in the beginning, the amplitude in the three variables decreases slightly from one event to the next, but after a while, the amplitude stays constant. ~~The system reaches~~ Therefore, it seems that the system asymptotically approaches a limit cycle ~~, through which it passes over and over periodically~~(one-dimensional attractor). This kind of scenario was also observed in former studies (e.g. Spichtinger and Cziczo, 2010; Kay et al., 2006) ~~.~~ but not in a long term behaviour.

Obviously, we find two qualitatively different states in the numerical solution of the model, depending on parameters w and T, respectively. Next, we investigate the model by means of qualitative theory of dynamical systems.

~~In the following section, we conduct a classical dynamical system analysis of the ODE system .Then, we discuss the properties of the modeled cloud~~

3.2 Qualitative behaviour of the model

For a first investigation we discuss the different terms in equations (25).

The model is driven by an external source; vertical lifting of the air parcel leads to increase of relative humidity. Since temperature and pressure are kept constant, the term $e \cdot w \cdot RH_i$ implies a permanent water vapour source, which is necessary for studying the long term behaviour of the model. The artificially produced water vapour leads to particle generation. Thus, the terms of nucleation and growth can be seen as internal transformation terms. Finally, sedimentation terms, i.e. $-b \cdot N_c^{1-\delta} q_c^{\delta}$ and ~~compare it to other models and observations.~~ $-c \cdot N_c^{-\delta} q_c^{\delta-1}$, remove particles (and thus water mass) from the model, so they constitute internal sinks for cloud variables. Qualitatively, the external sources of water initiate particle generation; diffusional growth terms transform water vapour mass into cloud mass until the mass is lost by the internal sinks of sedimentation. Thus, the model can be seen as an **externally forced dissipative system**. Note, that the model does not fulfil mass conservation due to the sources and sinks of water vapour and cloud mass, respectively. All terms except of the cooling term $e \cdot w \cdot RH_i$ are non-linear in variables N_c, q_c, RH_i.

For a first analysis we compute the divergence of the system (i.e. the trace of the Jacobian $\mathbf{DF}$):

$$\begin{aligned} \nabla \cdot \boldsymbol{F} &= -\left[(b(1-\delta)+c(1+\delta))N_c^{-\delta} q_c^{\delta} + f N_c^{1-\alpha_i} q_c^{\alpha_i}\right] + e \cdot w + d\alpha_i (RH_i - 100\%) N_c^{1-\alpha_i} q_c^{\alpha_i - 1} \\ &= -\left[(b(1-\delta)+c(1+\delta))\overline{m}^{\delta} + f N_c \overline{m}^{\alpha_i}\right] + e \cdot w + d\alpha_i (RH_i - 100\%) \overline{m}^{\alpha_i - 1} \end{aligned} \tag{27}$$

using the mean mass $\overline{m} = q_c / N_c$ for cloudy states. For clear air ($N_c = q_c = 0$), we obtain $\nabla \cdot \boldsymbol{F} = e \cdot w > 0$, hence the system is expanding in phase space. For cloudy air ($\overline{m} \neq 0$) there is competition between different terms determining the sign of $\nabla \cdot \boldsymbol{F}$. Sedimentation and change of relative humidity due to diffusional growth are dissipative terms (i.e. negative sign in equation (27)), while the external source

term always has a positive sign. Diffusional growth of ice particles can change its sign depending on the thermodynamic state. Since we always investigate a situation with $w > 0$, the system stays in a supersaturated states ($RH_i - 100\% > 0$), therefore the last term in equation (27) is positive.

The balance of terms in equation (27), i.e. the sign of $\nabla \cdot \boldsymbol{F}$ for cloudy air is crucially determined by the mean mass of the cloud. Note that for both exponents we have $0 < \alpha_i < \delta < 1$, and thus $-1 < \alpha_i - 1 < 0$. For large ice crystal mass, the terms of form $\overline{m}^{\delta}$ will dominate, thus leading to a negative sign of $\nabla \cdot \boldsymbol{F}$ and to dissipation of the system, mainly due to sedimentation of ice crystals. This is especially the case at higher temperatures, since then diffusional growth is faster and mean masses $\overline{m}$ tend to larger values. In such cases, the system tends to state 1.

For very small ice crystals, the term including $\overline{m}^{\alpha_i - 1}$ will dominate leading to a positive sign of $\nabla \cdot \boldsymbol{F}$. For instance, at nucleation events, the ice crystal mass becomes very small, thus in this situation the system tends to expand explosively ($\nabla \cdot \boldsymbol{F} > 0$). The same is true if almost all particles have fallen out and only small ice crystals are contained in the air parcel. These scenarios are more prevalent at state 2, i.e. at lower temperatures and higher upward velocities.

3.3 ~~Mathematical analysis~~Linear stability of the system

In a first step, the dynamical system (25) can be characterised by its critical points $\boldsymbol{x_0}$, i.e. the ~~values~~ points in phase space where $\boldsymbol{F}(\boldsymbol{x_0}) = \boldsymbol{0}$. Since the system is autonomous the critical or singular points are equilibrium ~~points. The critical points of the~~ states of the system. The equilibrium points of this system cannot be determined analytically~~. However, under the assumption that the nucleation term NUC_q for q_c is negligible (it is several orders of magnitude smaller than the other terms in equation), it is possible to rearrange the equations (without losing any positive solutions) in a way that only one equation for RH_i has to be solved numerically. The critical~~, due to strong nonlinearities. We determine the roots of the right hand side of system (25) numerically. First, we observe that the mass rate of nucleation $\frac{\mathrm{d}q_c}{\mathrm{d}t}\big|_{\text{nucleation}} = a \cdot m_0 \cdot J(RH_i, T)$ is negligible compared to other mass rates in the system and can be omitted for simplification. This leads to a new system $\dot{\boldsymbol{x}} = \tilde{\boldsymbol{F}}(\boldsymbol{x})$. After setting $\tilde{\boldsymbol{F}}(\boldsymbol{x}) = 0$, the three resulting equations can be combined to a single equation for RH_i as follows:

$$a \cdot J(RH_i, T) = \frac{e \cdot w \cdot b}{f} \cdot \left(\frac{d}{c}\right)^{\frac{\delta - \alpha_i}{\delta + 1 - \alpha_i}} \cdot RH_i \cdot (RH_i - 100\%)^{\frac{1}{\alpha_i - 1 + \delta}}. \tag{28}$$

For details of the derivation of this equation see appendix C. The roots of equation ((28)) determine the equilibrium values of RH_i. Then, the values of N_c and q_c can be derived analytically~~from that.~~

~~This equation reads:~~

$$\frac{4\pi}{3}\frac{n_a}{\rho}r_m^3\exp\left(\frac{1}{2}\left(3\ln(\sigma_r)\right)^2\right)J(RH_i,T)$$

$$= \frac{\gamma c(T,p) g w M_{air}\left(L_{ice}/c_p - 1\right)}{\Delta z R T \pi \rho C_i} \cdot r_0^{\frac{\delta}{2}(\delta-1)(\alpha_i-1)-\frac{\alpha_i}{2}(\alpha_i-1)}$$

$$\cdot\left(\frac{\pi\epsilon\rho D_v C_i e_i \Delta z}{\gamma c(T,p) p_i}\cdot\left(\frac{RH_i}{100\%}-1\right)\right)^{\delta-\alpha_i}\frac{RH_i}{RH_i - 100\%}.$$

~~Equation~~. Equation (28) has a unique solution because the left-hand side is a strictly monotonic increasing function of ~~RH_i~~ RH_i and the right-hand side is strictly monotonic decreasing. Therefore, there exists a unique critical point, $\boldsymbol{x_0}$, in the relevant domain of the phase space (~~$RH_i > 100\,\%$~~$RH_i > 100\,\%$, $N_c > 0$, $q_c > 0$). The roots of equation (28) are determined numerically for the relevant domain in the parameter space, i.e. $0 < w \leq 0.05\ \mathrm{m\,s^{-1}}$ and $190 \leq T \leq 235\ \mathrm{K}$.

In order to examine the qualitative behaviour of the solution in a neighbourhood of the equilibrium state, the ODE system is linearised about the critical point $\boldsymbol{x}_0$:

$$\dot{\boldsymbol{x}} = \boldsymbol{F}(\boldsymbol{x_0}) + \mathbf{DF}\big|_{\boldsymbol{x}_0}(\boldsymbol{x} - \boldsymbol{x}_0) + \mathcal{O}(|\boldsymbol{x} - \boldsymbol{x}_0|^2), \tag{29}$$

where $\mathbf{DF}|_{\boldsymbol{x}_0}$ is the Jacobian of $\boldsymbol{F}$ evaluated at ~~the point~~ $\boldsymbol{x}_0$. Note that $\boldsymbol{F}(\boldsymbol{x_0}) = 0$ by definition. The three eigenvalues of the Jacobian, $\lambda_1, \lambda_2, \lambda_3$, determine the quality of the critical point (Verhulst, 1996, Chapter 3). The eigenvalues must be determined numerically for the relevant parameter values w and T. The Jacobian of the system has two complex conjugate eigenvalues, ~~λ_1 and λ_2~~$\lambda_{1,2} \in \mathbb{C}$, whose real part can be positive or negative, depending on the parameters, w and T. In figure 3 the values of the real part $\mathrm{Re}(\lambda_{1,2})$ and the absolute value of the imaginary part $|\mathrm{Im}(\lambda_{1,2})|$ are shown. The third eigenvalue, $\lambda_3 \in \mathbb{R}$, is always negative, values are shown in figure 4.

~~If~~ Complex eigenvalues of the linearised system indicate oscillatory behaviour, which is prevalent in all simulations. As can be seen in figure 3, the real part of the complex ~~conjugate eigenvalues is negative ($\mathrm{Re}(\lambda_1) = \mathrm{Re}(\lambda_2) < 0$) ,~~ eigenvalues $\lambda_{1,2}$ can change its sign depending on parameters w and T.

For negative values of the real part ($\mathrm{Re}(\lambda_{1,2}) < 0$) the critical point $\boldsymbol{x}_0$ is a positive attractor~~in equation , which means that a solution that starts~~ , i.e. solutions of the ODE (29) starting in a neighbourhood of ~~$\boldsymbol{x_0}$ will asymptotically converge to $\boldsymbol{x_0}$ (Verhulst, 1996) . This corresponds to state 1, i.e. the damped oscillation where the system reaches stationarity~~this point approach this point asymptotically (Verhulst, 1996, Chapter 2) . More precisely, this equilibrium point can be characterised as stable focus (e.g. Verhulst, 1996; Argyris et al., 2010) . According to the Poincaré-Lyapunov theorem (Verhulst, 1996, theorem 7.1), positive attraction in the linearised system is also valid for the full ~~non-linear system~~ nonlinear system (25). Therefore, $\boldsymbol{x_0}$ is asymptotically stable and acts as a positive point attractor in equation ~~in state~~(25).

This equilibrium point (stable focus) corresponds to state 1 ~~(damping state)~~ in the numerical simulations. Solutions of the system (25) experience damped oscillations until they asymptotically approach the stable attractor in phase space. The imaginary part of the complex eigenvalues determines the oscillation period. Figure 5 shows the trajectory of a solution of the system (25) in the 3D phase space, spiralling towards the equilibrium point, i.e. the positive attractor.

~~In case of undamped oscillation (state 2), the real part of the complex eigenvalues is positive ($\mathrm{Re}(\lambda_1) = \mathrm{Re}(\lambda_2) > 0$).~~

For positive values of the real part ($\mathrm{Re}(\lambda_{1,2}) > 0$) the critical point $\boldsymbol{x}_0$ is a negative point attractor (unstable focus). Solutions starting in a neighbourhood of $\boldsymbol{x}_0$ run away from the unstable equilibrium point. In this case, the characterisation of an unstable critical point in the linearised system is not sufficient for a general characterisation of the full nonlinear system, since after short time the solutions are too far away from the equilibrium points. Numerical integration shows undamped oscillations for solutions that do not start in the equilibrium point; this behaviour points to the possibility of a limit cycle (one-dimensional attractor). The transition from positive point attractor to limit cycle is a so called Hopf bifurcation (Verhulst, 1996) and is associated with a transition from two conjugate complex eigenvalues with negative real part to two conjugate complex eigenvalues with positive real part, via two purely imaginary eigenvalues. ~~The bifurcation diagram is a line in w-T-space that separates the two regimes positive attraction vs. limit cycle (see figure 7). The bifurcation points were identified numerically using the eigenvalue criterion, $\mathrm{Re}(\lambda_1) = \mathrm{Re}(\lambda_2) = 0$.~~

~~The limit cycle was determined numericallyby computing~~ For vanishing real part of $\lambda_{1,2}$, the Hopf bifurcation occurs. The existence of a limit cycle cannot be shown analytically for this system; however, we can determine the limit cycle numerically. For this purpose, we compute the Poincaré map of the system (Argyris et al., 2010; Verhulst, 1996). ~~Choose~~ We choose a two-dimensional plane Σ in ~~the~~ phase space, which is transverse to the trajectory of the solution of equation (26); Σ is called Poincaré section. The sequence of points in ~~the~~ phase space where the trajectory crosses Σ converges numerically to the the point on the limit cycle that is in Σ. Once we find one such a point on the limit cycle, we can use it as the initial condition in (26) to compute the complete limit cycle. ~~However, since this method requires numerical integration of equation , it is not of further interest for the analytical investigation~~An example of a Poincaré section for determining the respective limit cycle is shown in appendix D (figure 16). The limit cycle itself constitutes a one-dimensional positive attractor, i.e. solutions starting outside of the limit cycle approach the limit cycle asymptotically. Figure 6 shows the trajectory of a solution of the system (25) in the 3D phase space, approaching the limit cycle, which constitutes a warped circle in phase space.

The transition between the two general states of the system (stable point attractor vs. limit cycle) can be represented in a bifurcation diagram of the w-T-space (figure 7). The bifurcation point is

a function of both w and T. The different states are separated by points with vanishing real part of eigenvalues $\lambda_{1,2}$, indicated by the thick black line. The bifurcation points were obtained numerically.

3.4 ~~Discussion of results~~Quantitative overview

After discussing the different states of the system qualitatively, we now give an overview of the quantitative cloud properties and relative humidity for the point attractor and the limit cycle, respectively.

In the "point attractor" regime (stable focus), i.e. ~~state 1~~ **state 1** of the system, the critical point corresponds to the equilibrium values within the finally persisting cloud. Hence, in this parameter regime, we describe the properties of the modeled cloud by the values of the system variables at the critical point. For the "limit cycle" regime, i.e. **state 2** of the system, the critical point does not describe the changing properties of the cloud since it is only in the centre of the periodic orbit and the trajectory does not approach it. A more revealing measure for the cloud properties in this regime is a probability density of the values the variables take ~~in~~ along the limit cycle, or at least median, maximum and minimum values.

Figure 8 shows ice crystal mass and number concentrations, respectively, at the critical point, $\boldsymbol{x_0}$, as a function of vertical velocity ($q_c(w)$, $N_c(w)$) for different temperature regimes. The solid lines in both panels correspond to state 1 (~~attractor regime~~point attractor regime, damped oscillations), whereas the dashed lines indicate the values at the critical point, $\boldsymbol{x_0}$, for state 2 (limit cycle regime, undamped oscillations); note that for state 2, $\boldsymbol{x_0}$ is an unstable focus.

Ice crystal number concentrations at the critical point take values in the range ~~$3 \times 10^2\,\mathrm{kg}^{-1} \leq N_c \leq 2 \times 10^5\,\mathrm{kg}^{-1}$~~ $3 \times 10^2\ \mathrm{kg}^{-1} \leq N_c \leq 2 \times 10^5\ \mathrm{kg}^{-1}$ (figure 8, top), which corresponds to ice crystal number densities of ~~$0.1\,\mathrm{L}^{-1} \leq n_c \leq 110\,\mathrm{L}^{-1}$~~ $0.1\ \mathrm{L}^{-1} \leq n_c \leq 110\ \mathrm{L}^{-1}$. Ice crystal mass concentration ranges between ~~$4 \times 10^{-9} \leq q_c \leq 3 \times 10^{-6}\,\mathrm{kg\,kg}^{-1}$~~ $4 \times 10^{-9} \leq q_c \leq 3 \times 10^{-6}\ \mathrm{kg\,kg}^{-1}$ (figure 8, bottom). This corresponds to an ice water content of ~~$2.2 \times 10^{-9} \leq IWC \leq 1.4 \times 10^{-6}\,\mathrm{kgm}^{-3}$~~ $2.2 \times 10^{-9} \leq IWC \leq 1.4 \times 10^{-6}\,\mathrm{kg\,m}^{-3}$.

As expected from theory (e.g. Kärcher and Lohmann, 2002) and from former numerical investigations ~~(e.g. Kärcher and Lohmann (2002))~~(e.g. Spichtinger and Gierens, 2009) , the ice crystal number concentrations display a strong increase with rising vertical velocity. Due to increased crystal growth rates at higher temperatures, N_c decreases with rising T.

In the double logarithmic representation in figure 8, the number concentrations $N_c(w)$ at $\boldsymbol{x_0}$ appear as straight lines. For different temperature regimes, there seems to be a constant shift between the curves $N_c(w)$~~(i.e. a constant factor c(T))~~, leading to parallel lines in the double logarithmic representation.

For the limit cycle regime (state 2), we can still derive the values of mass and number concentrations at the critical point, $\boldsymbol{x_0}$. However, since this point is ~~unstable and is never reached~~an unstable focus, another representation is needed to describe the range of ice crystal concentrations. As indicated in figures 7 and 8, the limit cycle behaviour occurs for temperatures $T < 230\,\mathrm{K}$ for

the investigated updraught regime $0 \leq w \leq 0.05\,\mathrm{ms}^{-1}$. Thus, in figure 9 we ~~represent maximum , median~~ present maximum and minimum values (dashed lines) and median values (dot-dashed lines) for ice crystal number concentrations ~~(dashed lines)~~ in the limit cycle regime for temperatures $T = 190, 200, 210, 220\,\mathrm{K}$. In addition, the ice crystal number concentration at the critical point, $\boldsymbol{x_0}$, is displayed (solid lines). We observe a large variation in the number concentrations of up to two orders of magnitude relative to the median. This behaviour is reasonable since sedimentation reduces the amount of ice crystals in a dominant manner, while new ice crystals are formed by nucleation in a pulsating way. The absolute values are in the range $0.2 \leq n_c \leq 200\ \mathrm{L}^{-1}$.

The mass concentration of the ice crystals is largely determined by the efficiency of diffusional growth. As indicated in the model description (section 2), this term depends on temperature and also on number concentration, leading again to ~~an exponential behaviour~~ a power law relationship as represented in figure 8 (bottom) and to a constant ~~factor~~ shift between the different temperatures, represented as parallel lines.

For the point attractor regime, we can directly investigate the mean mass of the ice crystals, $\overline{m} = q_c/N_c$, at $\boldsymbol{x_0}$, which is displayed in figure 10. The variation of $\overline{m}$ at the critical point due to the vertical velocity is marginal, as indicated in the figure. Thus, we can assume that $\overline{m}$ can be approximated by a function of temperature. The mean mass at $\boldsymbol{x_0}$ ranges between $\overline{m} \sim 10^{-12}\,\mathrm{kg}$ and $\overline{m} \sim 2 \times 10^{-10}\,\mathrm{kg}$, which corresponds to mean sizes between $\overline{L} \sim 16\,\mu\mathrm{m}$ and $\overline{L} \sim 134\,\mu\mathrm{m}$. For the limit cycle regime (state 2), we indicate the variation in the mean mass by box and whiskers plots, displaying the median value (red markers) as well as 25/75% percentiles and minimum/maximum values. Note here that variation of mean mass is usually of one order of magnitude. For cold temperatures the variation is larger due to a higher variability in ice crystal number concentration (see figure 9), whereas the mass concentration in ice clouds is mainly dominated by available water vapour.

As indicated in section 3.3, the imaginary part of the complex eigenvalues $\lambda_{1,2}$ determines the period of the oscillations in state 1 near the equilibrium point. In figure 11 the period $\tau = \frac{2\pi}{\mathrm{Im}(\lambda_{1,2})}$ as calculated from the imaginary part is shown for the stable focus (solid lines, colours indicate different temperature regimes). For the unstable focus, the imaginary part of the eigenvalues is not meaningful, as the limit cycle is not within the linear regime of $\boldsymbol{x_0}$. Instead, the periods of the limit cycle is shown (dashed lines, colours indicate different temperature regimes) as calculated from the Poincaré map. Note that for decreasing temperature the period τ becomes very large.

3.5 Comparison with ~~other simulations~~observations

For comparison with ~~a more complex and realistic model we carry~~ observations we first consider in situ measurements of ice crystals in subvisible cirrus clouds. Since it is very difficult to measure low number concentrations, only few measurement studies are available. We compare our results with measurements by Kübbeler et al. (2011) , Lawson et al. (2008) and Davis et al. (2010) .

Our model results lead to ice crystal number concentrations in the range $0.1\,\mathrm{L}^{-1} \leq \rho N_c \leq 200\,\mathrm{L}^{-1}$ and mean ice crystal sizes in the range $\sim 16\,\mu\mathrm{m} \leq \overline{L} \leq 134\,\mu\mathrm{m}$. Note, that the variation in number concentrations span over three orders of magnitude and the variation in mean sizes is still within two orders of magnitude. These values agree quite well with the measurements. Kübbeler et al. (2011) observed quite high number concentrations in order of $\sim 100\,\mathrm{L}^{-1}$ for small ice crystals ($L \sim 10\,\mu\mathrm{m}$) but quite low number concentrations $0.1 \leq \rho N_c \leq 10\,\mathrm{L}^{-1}$ for large ice crystals (equivalent radius $r > 50\,\mu\mathrm{m}$). Lawson et al. (2008) reported ice crystal number concentrations in the range $22.5 \leq \rho N_c \leq 188.8\,\mathrm{L}^{-1}$ with mean value and standard deviation $66 \pm 30.8\,\mathrm{L}^{-1}$ for ice crystals in the size range $1 \leq L \leq 200\,\mu\mathrm{m}$. Finally, Davis et al. (2010) reported very low ice crystal number concentrations with a mean value of $2\,\mathrm{L}^{-1}$ and mean sizes of $14\,\mu\mathrm{m}$ during the tropical measurement campaign TC4. However, in their study values from former measurement campaigns are reported to be in the range $10 \leq \rho N_c \leq 100\,\mathrm{L}^{-1}$ and for effective radii $10 \leq r \leq 20\,\mu\mathrm{m}$. In a second step we expand our comparison to observations from remote sensing. Since SVCs are optically very thin, we investigate the extinction coefficient for the visible part of the spectrum. For comparing our results with measurements, we calculate the extinction β in the solar range using parameterisations by Fu and Liou (1993) :

$$\beta = IWC \cdot \left(a + \frac{b}{D_e} \right), \tag{30}$$

where $IWC = q_c \cdot \rho$ denotes ice water content in $\mathrm{g\,m}^{-3}$ and D_e is the generalised size. Constants are given by $a = -6.656 \cdot 10^{-3}\ \mathrm{m^2 g^{-1}}$ and $b = 3.686\ \mu\mathrm{m\,m^2 g^{-1}}$. As a useful approximation we set $D_e = \overline{L}$, where the quantity $\overline{L}$ is calculated from the mean mass $\overline{m}$ using the mass-length-relation $\overline{L} = C_i \overline{m}^{\alpha_i}$, as indicated in appendix B. In figure 12 the values for β are shown for different temperature regimes as calculated for the mean values at the (stable and unstable) focus (equilibrium point). Note that there is only marginal difference in the values for different temperatures. The values are within the interval $10^{-4} \leq \beta \leq 0.02\ \mathrm{km}^{-1}$.

Seifert et al. (2007) report mean values for extinctions of SVCs in the range $0.015 \leq \beta \leq 0.02\,\mathrm{km}^{-1}$ with standard deviations $\sigma \sim 0.005 - 0.009\,\mathrm{km}^{-1}$ (see their table 3). Our results are in the same order of magnitude or even smaller for slow vertical updraughts. Davis et al. (2010) report much smaller values of extinction scattered in the range $0 < \beta < 0.01$ with a mean value of $\overline{\beta} \sim 0.001\ \mathrm{km}^{-1}$. These SVCs were measured in the tropics at high altitudes ($z \sim 16\ \mathrm{km}$), i.e. at low temperatures $T < 195\,\mathrm{K}$, where slow large-scale updraughts due to Kelvin waves in order of $w < 0.01\ \mathrm{m\,s}^{-1}$ dominate (Immler et al., 2008b) . This is consistent with our results, see figure 12.

Overall, we can state that regarding the high spread in the measurements our results from a simple analytical model agree quite well with in situ measurements.

3.6 Comparison with other models

For comparison with a more detailed model we carried out simulations with the ~~boxmodel as~~ box-model described by Spichtinger & Gierens (2009) and Spichtinger & Cziczo (2010). ~~In the following~~

This model includes more sophisticated treatment of microphysical processes, although it is also a two-moment bulk model. It allows a change in the shape of ice crystals from almost spherical droxtals to columns. Homogeneous nucleation is treated in detail, including deliquescence of sulphuric acid and integration over the full size distribution of solution droplets. For diffusional growth, kinetic and ventilation effects are included. Finally, temperature and pressure changes due to vertical upward motions and latent heat release is added to the air parcel's temperature.

Henceforth this model is termed "complex model". We scan through the T-w parameter space using initial temperatures in the range $190 \leq T \leq 235\,\mathrm{K}$ with a temperature increment of ~~$\Delta T = 5\,\mathrm{K}$~~ $\Delta T = 5\,\mathrm{K}$ and vertical velocities in the range ~~$0.005 \leq w \leq 0.05\,\mathrm{ms}^{-1}$~~ $0.005 \leq w \leq 0.05\,\mathrm{m\,s}^{-1}$ with a velocity increment of ~~$\Delta w = 0.005\,\mathrm{ms}^{-1}$~~ $\Delta w = 0.005\,\mathrm{m\,s}^{-1}$, leading to 90 simulations. Additionally, we fixed initial conditions ~~$p = 300\,\mathrm{hPa}$ and $RHi = 140\%$. The~~ $p = 300\,\mathrm{hPa}$ and $RH_i = 140\%$. Generally, the results of these simulations are ~~very similar to~~ in good agreement with the results of the analytical model.

We can again identify regimes in the T-w parameter space showing the known two different states, i.e. damped oscillations (state 1) and limit cycle behaviour (state 2). In figure 13 the case of damped oscillation is shown in both model simulations. Here, initial temperature of $T = 220\,\mathrm{K}$ is used with a vertical velocity of ~~$w = 0.01\,\mathrm{ms}^{-1}$~~ $w = 0.01\,\mathrm{m\,s}^{-1}$. Green lines indicate the evolution in the complex model simulation, whereas blue lines represent the evolution in the simple analytical model. ~~Both model simulations agree quite well.~~ For the variables number and mass concentration, both models produce almost the same values~~, however the values for relative humidity are slightly lower for the simple model simulation. In fact, the~~. The onset of ice nucleation is shifted between the two models due to differently detailed representation of ice nucleation in both models. This leads to the difference in relative humidity values. Qualitatively, the models agree very well ~~,~~ the oscillation periods ~~are very similar and also the damping is almost the same. Note that the agreement between the models is not always that good for all parameter values; however, the model results for variables ice mass and number concentrations, respectively, always agree within less than one order of magnitude~~and the magnitudes of the damping are very similar.

For the complex model simulations the environmental conditions change, i.e. temperature and pressure are decreasing due to adiabatic expansion. Thus, no steady state can be reached. The values for ice crystal number concentrations and relative humidity are slightly rising with time in the quasi steady state at the end of the simulation. Ice crystal mass concentration is slightly decreasing. ~~Generally, we can say that for state 1 (damped oscillations) the agreement between the respective two model simulations is very good; this holds for all cases of damped oscillations.~~

In figure 14, a case of limit cycle behaviour is shown. As in figure 13, green lines indicate the complex model simulations and the simple model results are represented by blue lines, respectively. The initial conditions for both models are given by $T = 210\,\mathrm{K}$ and ~~$w = 0.02\,\mathrm{ms}^{-1}$~~ $w = 0.02\,\mathrm{m\,s}^{-1}$. Again, we find very good agreement in the cloud variables ~~N_c, q_c~~ N_c, q_c between both model sim-

ulations. ~~There is again a shift in relative humidity due to the representation of ice nucleation in the different models. The limit cycle behaviour is present in both simulations; qualitatively~~ Qualitatively they also agree very well in terms of the periods of the oscillations. ~~Again, we have to state that the agreement is not always that good in the absolute values of variables as in this represented case. However, qualitatively the limit cycle cases agree very well.~~

The bifurcation diagram ~~as represented~~ displayed in figure 7 cannot ~~completely be reproduced~~ be reproduced accurately by the complex simulations. ~~For initial conditions close to the boundary between state 1 and state 2 we observe a different behaviour. Since~~ Since in the complex model ~~includes changes in temperature, the parameters are~~ the parameter T is changed during the simulations~~. For instance, the simulation starts in the regime of a damped oscillation~~ , switching from one regime to the other is possible within one simulation. If, for instance, a simulation starts at a point in parameter space within the point attractor regime (e.g. high temperature ~~vales~~ at low updraughts)~~and~~ , the time evolution ~~follows first this (theoretical) kind of time evolution~~initially follows the damped oscillations as expected from the bifurcation diagram of the simple model. However, the temperature change leads to a (horizontal) path in the phase diagram (figure 7) and at some stage the boundary between the two states is crossed~~. Now, a different scenario, namely limit cycle behaviour, should be present. In fact, if the oscillations are not already damped out, we can observe in~~ , and from then on, the ~~simulations that after crossing the bifurcation line in figure 7 the~~ system will perform undamped oscillations. Indeed, we observe this transition in the complex model simulations~~then exhibit a limit cycle behaviour~~. An example for this situation is given in figure 15~~. Here, we show a long simulation with the complex model for~~ , with initial conditions $T = 225\,\mathrm{K}$ and ~~$w = 0.035\,\mathrm{ms}^{-1}$; thus, as shown in the phase diagram (figure 7), the model starts in the regime of damped oscillations. In the time evolution, we can see the damped oscillation very clearly for up to about four hours. At this time, the temperature is about $T \sim 220\,\mathrm{K}$ and according to the phase diagram there is the transition to~~ $w = 0.035\,\mathrm{m\,s}^{-1}$. Note that in the limit cycle ~~behaviour. In the further time evolution, the limit cycle behaviour is present, i.e. the oscillations are not damped but in contrast the amplitude in variables N_c, q_c and relative humidity increases slightly. After further cooling, we observe that the period~~ regime the properties of the theoretically expected limit cycle also change with decreasing T. This results in increasing amplitudes of the oscillations ~~changes as well, since the period of the limit cycle depends on environmental conditions~~in N_c, q_c, RH_i and in increasing periods. Thus, we can conclude that for realistic simulations including changes in environmental conditions there could be transitions between the theoretically determined states. However, the behaviour of the actual states can still be explained by the phase diagram as obtained from our analytical considerations.

We also compare our results with the analytical model Kärcher (2002) . This model includes a more sophisticated representation of nucleation and growth. The relevant equations are treated using typical time scales and approximation of the occuring intergrals. Comparison with theoretical results by Kärcher (2002) shows good agreement as well. Actually, in our investigations with the simple an-

alytical model we found low ice crystal number concentrations similar to results by Kärcher (2002); the dependence of number concentrations on w and T also agrees very well with analytical considerations by Kärcher (2002). However, our approach goes beyond the results by Kärcher (2002) since we allow for sedimentation of ice crystals. This additional process leads to the oscillatory behaviour in both ~~cases, the damped oscillation in the attractor case (state 1) as well as the undamped oscillation in the limit cycle case (state 2)~~states, whereas in the study by Kärcher (2002) a steady state at ice saturation is reached soon. Especially the continuous nucleation in the state 1 scenario (damped oscillation) is only possible if we allow for sedimentation of ice crystals. Otherwise, the nucleation event would stop after depositional growth has reduced the supersaturation such that nucleation rates become negligible. Thus, we can state that our scenarios might be more realistic, although the microphysical ~~poperties~~ properties in both studies are quite similar.

3.7 ~~Comparison with observations~~

~~For comparison with observations we focus on in situ measurements of ice crystals in subvisible cirrus clouds. Since it is very difficult to measure low number concentrations, only few measurement studies are available. We compare our results with measurements by Kübbeler et al. (2011) , Lawson et al. (2008) and Davis et al. (2010) .~~

~~Our model results lead to ice crystal number concentrations in the range $0.1\,\mathrm{L}^{-1} \leq \rho N_c \leq 110\,\mathrm{L}^{-1}$ and mean ice crystal sizes in the range $\sim 16\,\mu\mathrm{m} \leq \overline{L} \leq 134\,\mu\mathrm{m}$. Note, that the variation in number concentrations span over three orders of magnitude and the variation in mean sizes is still within two orders of magnitude. These values agree quite well with the measurements. Kübbeler et al. (2011) indicated quite high number concentrations in order of $\sim 100\,\mathrm{L}^{-1}$ for small ice crystals ($L \sim 10\,\mu\mathrm{m}$) but quite low number concentrations $0.1 \leq \rho N_c \leq 10\,\mathrm{L}^{-1}$ for large ice crystals (equivalent radius $r > 50\,\mu\mathrm{m}$). Lawson et al. (2008) reported ice crystal number concentrations in the range $22.5 \leq \rho N_c \leq 188.8\,\mathrm{L}^{-1}$ with mean value and standard deviation $66 \pm 30.8\,\mathrm{L}^{-1}$ for ice crystals in the size range $1 \leq L \leq 200\,\mu\mathrm{m}$. Finally, Davis et al. (2010) reported very low ice crystal number concentrations with a mean value of $2\,\mathrm{L}^{-1}$ and mean sizes of $14\,\mu\mathrm{m}$ during the tropical measurement campaign TC4. However, in their study values from former measurement campaigns are reported to be in the range $10 \leq \rho N_c \leq 100\,\mathrm{L}^{-1}$ and for effective radii $10 \leq r \leq 20\,\mu\mathrm{m}$. Overall we can state that regarding the high spread in the measurements our results from a simple analytical model agree quite well with in situ measurements.~~

~~Actually, from in situ measurements, which constitute an Eulerian point of view by definition, we cannot decide in which of the possible states (attractor regime vs. limit cycle) the observed cloud might be. We also have to keep in mind that in reality the motion of air parcels might be disturbed by small scale turbulence or other dynamical effects.~~

4 Conclusions

In this study we ~~develop~~ developed an analytical model for describing subvisible cirrus clouds formed by homogeneous nucleation in the tropopause region~~from first principles starting with a Boltzmann-type equation for the evolution of a cloud mass distribution~~. The model consists of a set of autonomous ordinary differential equations for the variables ice crystal mass and number concentration~~as well as~~ , and relative humidity with respect to ice. ~~The model~~ It contains the relevant cloud processes ice nucleation, diffusional growth and sedimentation~~, respectively. The forcing terms are non-linear and the whole systemis autonomous. We use this model for numerical simulations as well as for mathematical analysis, applying~~ . The model can be viewed as an externally forced dissipative system. The model is integrated numerically and also investigated using linear theory of dynamical systems. ~~In the analysis we can show that there are two qualitatively different states in the long-term evolution of the model. The two states are (a) a positive attractor and (b)~~

Integration and theoretical analysis show that the system contains two different states, a point attractor state and a limit cycle ~~for the cloud variables. Thus, we find a Hopf bifurcation, which is characterized by the change of the real part of the two conjugate-complex eigenvalues from negative values to positive values via two purely imaginary eigenvalues. The transition between the states is determined by the parameters vertical velocity~~ state. The states depend on the environmental parameters vertical updraught, w~~and environmental temperature~~, and temperature, T. The transition between the states can be described as Hopf bifurcation. Both states show oscillatory behaviour, either damped (point attractor) or basically undamped (limit cycle).

The microphysical properties of the cloud in both states ~~are similar and~~ depend mostly on the environmental conditions as vertical velocity and temperature. However, for the limit cycle case the spread in ice crystal mass and number concentration is obviously larger than in the attractor case. For the ~~equilibrium point~~ stable point attractor, the mean mass depends only slightly on vertical velocity, thus we can approximate the mean mass as a function of temperature.

~~The comparison with a complex boxmodel by Spichtinger and Gierens (2009) shows~~ Comparisons with a more detailed box-model by Spichtinger and Gierens (2009) show very good agreement. ~~In fact, the~~ The qualitative behaviour as determined for the analytical model can also be found for the complex model simulations. Also~~in a quantitative way~~ , in terms of quantitative results both models agree quite well.

~~Comparison with former~~ Former analytical investigations by Kärcher (2002) ~~shows also~~ show good agreement with our model, too. However, since we include sedimentation in our model, our results go clearly beyond the former investigations; the long-term behaviour is different, since the inclusion of sedimentation crucially leads to the bifurcation, depending on environmental conditions.

Since there are only ~~a~~ few in situ measurements of subvisible cirrus available, it is quite difficult to carry out solid comparisons. However, we try to compare with measurements as described by Kübbeler et al. (2011), Lawson et al. (2008), and Davis et al. (2010) and find good agreement with

our results. Also the extinction coefficient as calculated from model results agree very well with observations obtained with remote sensing techniques (Seifert et al., 2007; Davis et al., 2010) .

~~Thus, we can summarize~~ The major qualitative results can be summarised as follows:

- We could show that homogeneous freezing of aqueous solution droplets at low temperatures ($T < 235\,\mathrm{K}$) ~~might be a possible candidate for formation of ice crystals und slow updraught conditions, leading to very thin or~~ is a possible pathway for the formation of subvisible cirrus clouds at low vertical updraughts. Thus, the question about the dominance of formation mechanisms for these thin clouds remains open (homogeneous vs. heterogeneous nucleation).

- In unperturbed weak large scale updraughts subvisible cirrus clouds ~~. The final state of the cloud~~ can exist in two different qualitative states, reaching either an equilibrium point in the long term behaviour or experiencing oscillation behaviour in a limit cycle scenario. The state depends on external parameters as large-scale updraught and temperature, respectively.

- The cloud particle properties in the long-term behaviour ~~is~~ are very similar for both ~~cases~~states. Therefore, we cannot decide from values of microphysical properties in a certain range in which state the cloud might be. Even if we had more measurements, we probably would not be able to decide between the two states just using the Eulerian measurements without a Lagrangian point of view.

- The derived bifurcation diagram may be interpreted as a minimal model for subvisible cirrus clouds, i.e. a damped oscillator, which changes its eigenvalues depending to environmental parameters w and T, respectively, in a Hopf bifurcation.

We might derive a minimal model for SVCs from the bifurcation diagram in the following way. If we assume that SVCs are well approximated by their attractors, we could express cloud variables and relative humidity by a simple damped harmonic oscillator of the form

$$\ddot{x} + \kappa\dot{x} + \omega = 0, \tag{31}$$

with $x \in \{N_c, q_c, RH_i\}$ and parameters $\kappa = \kappa(w,T)$ and $\omega = \omega(w,T)$, respectively. κ describes damping, whereas ω represents oscillation frequency. κ, ω can be determined using eigenvalues λ_i for damping and oscillations in the point attractor case ($\kappa \neq 0$). For the limit cycle case ($\kappa = 0$), periods as obtained from the Poincaré section (see figure 11) can be used for describing ω. Such a minimal model could be used for representing SVCs in large-scale models and can be seen as a prototype for new generation cloud parameterisations. These models describe the structure of clouds in terms of cloud variables and environmental conditions. They could be used for describing such structures embedded into a coarse grid model. However, further research in this direction is necessary in order to proceed from pure model prototypes to useful cloud parameterisations.

Finally, we can state that we could develop a meaningful ~~minimal~~ simple model for describing the main features of subvisible cirrus clouds. Former investigations using ~~boxmodels~~ box-models indicated that there might be different regimes in the behaviour of the clouds for longer simulation times. For instance, in studies by Kay et al. (2006) and Spichtinger and Cziczo (2010) oscillatory behaviours as well as attractors could be seen. However, only a detailed mathematical analysis could show that there is a bifurcation in the long-term behaviour and that it depends mostly on environmental parameters as updraught velocity and temperature. This analysis was only possible ~~,~~since we developed an analytical model, which is close enough to complex models but is also simple enough for mathematical analysis.

The ~~determined Hopf bifurcation in addition with the~~ observed Hopf bifurcation as a transition between two different states ~~show~~ shows that clouds might ~~show~~ exhibit inherent structures, which are crucially determined by the microphysical cloud processes themselves in addition to environmental conditions. Similar structure formation was already seen in analytical cloud models for liquid and mixed-phase clouds as developed by Wacker (1992, 1995, 2006) or Hauf (1993). ~~Investigations~~ Investigation and analysis of the microphysical processes in terms of sets of ordinary differential equations are a first but urgently necessary step in order to investigate structure formation inside clouds. Once we understand the possible structures in clouds as determined by microphysics, we can ~~proceed further in order to investigate further~~ continue to further investigate structure formation as driven by ~~diffusion processes~~ spatial diffusion processes, mixing and others, leading to spatial structures of clouds. A first possible approach might be to investigate equations with additional spatial diffusion terms regarding possible Turing instabilities (Turing, 1952) . However, further research in this direction is necessary in order to investigate structure formation of ice clouds.

~~Last but not least we would like to note that simple models as the derived minimal model of subvisible cirrus cloudsmight also serve as prototypes for new generation of cloud parameterisations~~

Appendix A: Derivation of model equations

Splitting up the velocity as explained in section 2.1, $\boldsymbol{u}(m,\boldsymbol{x},t) = \boldsymbol{v}(\boldsymbol{x},t) + \boldsymbol{v}'(m,\boldsymbol{x},t)$, we adapt equation (1) accordingly:

$$\frac{\partial(\rho f)}{\partial t} + \nabla_x \cdot (\rho \boldsymbol{v} f) + \nabla_x \cdot (\rho \boldsymbol{v}' f) + \frac{\partial(\rho g f)}{\partial m} = \rho h. \tag{A1}$$

To derive equations for the evolution of moments, we multiply equation (A1) by m^k and integrate by parts, using $f(0,\boldsymbol{x},t) = 0$ and $f(m,\boldsymbol{x},t) \to 0$ for $m \to \infty$, which are physically reasonable assumptions.

This yields the following equation:

$$\frac{\partial(\rho\mu_k)}{\partial t} + \nabla_x \cdot (\rho \boldsymbol{v} \mu_k) + \nabla_x \cdot \left(\int_0^\infty m^k \rho \boldsymbol{v}' f \,\mathrm{d}m \right) = k \int_0^\infty m^{k-1} \rho g f \,\mathrm{d}m + \int_0^\infty m^k \rho h \,\mathrm{d}m, \qquad k \in \mathbb{R}. \tag{A2}$$

We allow generalised moments μ_k with $k \in \mathbb{R}_{\geq 0}$, which occur naturally from cloud physics parameterisations. Formally, the unit of the k-th moment is $\mathrm{kg}^k \mathrm{kg}^{-1}$. For simplicity, we assume the mass distribution to be horizontally homogeneous, i.e. $f = f(m, z)$.

Using $\boldsymbol{v}' = (0, 0, -v_t(m))$, and with the help of the continuity equation,

$$\frac{\partial \rho}{\partial t} + \nabla_x \cdot (\rho \boldsymbol{v}) = 0, \tag{A3}$$

the moment equation (A2) is rearranged to obtain equation (3).

Appendix B: Details of parameterisations

Nucleation

Homogeneous nucleation, i.e. the transformation of a solution droplet to an ice crystal, can be seen as a stochastic process. The transition rate ω for the transformation of a solution droplet of volume V can be expressed using a volume nucleation rate J, i.e. $\omega = V \cdot J$. The probability $P(t)$ for the nucleation process of droplets of volume V fulfil-ls the following differential equation:

$$\frac{\mathrm{d}P}{\mathrm{d}t} = -\omega P(t). \tag{B1}$$

For further details of the general derivation we refer to Koop et al. (1997) . Equation (B1) can be generalised for size distributions of solution droplets, leading to the formulation of equation (7).

Koop et al. (2000) provide a parameterisation for the volume nucleation rate J as a function of $\Delta a_w := a_w - a_w^i$ (Koop et al., 2000, Table 1, eq. 7) . Here a_w is the water activity of the solution and a_w^i is the water activity of the solution in equilibrium with ice. Note, that the freezing characteristics of the droplets do not depend on the chemical composition. By definition the water activity is the ratio p_{sol}/p_{liq} of the vapour pressure over a solution, p_{sol}, and pure liquid water, p_{liq}. Neglecting the Kelvin effect and assuming that the solution droplets are in equilibrium with the environment ($p_v = p_{sol}$), the water activity is proportional to the water activity in equilibrium with ice, which is the ratio of the water vapour pressure over ice and pure liquid water:

$$a_w = \frac{p_{sol}}{p_{liq}} = \frac{p_v}{p_{liq}} = \frac{RH_i}{100\%} \frac{p_{si}}{p_{liq}} = \frac{RH_i}{100\%} a_w^i. \tag{B2}$$

Both p_{si} and p_{liq}, only depend on temperature and are parameterised according to Murphy and Koop (2005, eq. 7 and 10, respectively).
Hence, Δa_w is a function of RH_i and T, as given by

$$\Delta a_w(T, RH_i) = \left(\frac{RH_i}{100\%} - 1\right) a_w^i(T) = \left(\frac{RH_i}{100\%} - 1\right) \frac{p_{si}}{p_{liq}}. \tag{B3}$$

Therefore J is also a function of RH_i and T. The logarithm of the nucleation rate is parameterised by a third order polynomial in Δa_w (Koop et al., 2000, table1, eq. 7) :

$$\log_{10} J(T, RH_i) = -906.7 + 8502\ \Delta a_w - 26924(\Delta a_w)^2 + 29180(\Delta a_w)^3. \tag{B4}$$

Diffusional growth

The "advection velocity" g in the mass space is given by the growth equation for a single ice crystal; this equation has the following form (see, e.g., Stephens, 1983) :

$$g(m) = \frac{\mathrm{d}m}{\mathrm{d}t} = 4\pi C D_v^* \rho (q_v - q_{v,si}) f_v. \tag{B5}$$

Here, $q_{v,si} = \varepsilon\, p_{si}(T)/p$ denotes the saturation mixing ratio, the shape of the ice crystal is accounted for by the capacity C (assuming the electrostatic analogy, see e.g. McDonald, 1963; Jeffreys, 1918) , D_v^* is the full diffusion constant including the kinetic correction for small particles (Lamb and Verlinde, 2011) and f_v denotes the ventilation coefficient.

In this study we make use of the following simplifications:

1. Latent heat release at the crystal surface is neglected and the temperature of the ice particles is assumed to be equal to temperature of ambient air.

2. We neglect kinetic corrections, since we are mostly interested in growth of larger crystals. Kinetic corrections are usually important for ice crystal growth in regimes with high concentrations of small crystals. For SVCs we can assume small concentrations, thus crystals will grow fast to sizes larger than $\sim 10\,\mu\mathrm{m}$. Thus, we can assume

   $$D_v^* \approx D_v = D_0 \left(\frac{T}{T_0}\right)^{\alpha} \left(\frac{p_0}{p}\right), \tag{B6}$$

   with $D_0 = 2.11 \cdot 10^{-5}\,\mathrm{m^2 s^{-1}}$, $T_0 = 273.15\,\mathrm{K}$, $p_0 = 101325\,\mathrm{Pa}$, $\alpha = 1.94$ (e.g. Pruppacher and Klett, 1997) .

3. We neglect correction of ventilation, setting $f_v = 1$. Ventilation correction is only relevant for very large crystals, so this is a reasonable assumption, since in SVCs ice crystals are usually smaller than $\sim 200\,\mu\mathrm{m}$.

4. The shape of ice crystals is assumed to be prolate spheroids with length L and an eccentricity ε', which leads to the following expression (McDonald, 1963) :

   $$C = L \frac{\varepsilon'}{\log\left(\frac{1+\varepsilon'}{1-\varepsilon'}\right)}. \tag{B7}$$

For the mass-length relation we assume a simple power law $L(m) = C_i m^{\alpha_i}$ using $C_i = 1.02\,\mathrm{m}$, $\alpha_i = 0.4$. This power law mostly represents the columnar shape of ice crystals, which is assumed for crystals with sizes $L > 10\,\mu\mathrm{m}$. The power law was fitted to a more complex description in Spichtinger and Gierens (2009) , where a transition between droxtals and columns is formulated and used.

The fraction in equation (B7) only depends weakly on the crystal mass and can be approximated by a constant mean value of $1/3$. This yields

$$C = \frac{1}{3} C_i m^{\alpha_i}. \tag{B8}$$

With these assumptions, equation (B5) can be approximated as follows:

$$g(m) \approx \frac{4}{3}\pi C_i D_v m^{\alpha_i} \rho (q_v - q_{v,si}) = \frac{4}{3}\pi C_i D_v m^{\alpha_i} \rho q_{v,si} (S_i - 1), \tag{B9}$$

leading to equation (11).

Sedimentation

The description of sedimentation is based on the concept of mass and number weighted terminal velocities defined by Spichtinger and Gierens (2009) . An expression for the sedimentation flux (i.e. the integral in the sedimentation term in equation (3)), can be found by applying the mean value theorem. Consider a mean velocity, $\bar{v}_k$, such that

$$\int_0^\infty v_t(m) \rho m^k f(m)\,\mathrm{d}m = \bar{v}_k \int_0^\infty \rho m^k f(m)\,\mathrm{d}m = \rho \bar{v}_k \mu_k. \tag{B10}$$

There exists a corresponding velocity for each moment of the distribution $f(m)$. For the double moment scheme, the number weighted terminal velocity (for the number flux), $\bar{v}_0 = \bar{v}_n$ $(k = 0)$ and the mass weighted terminal velocity (for the mass flux), $\bar{v}_1 = \bar{v}_q$ $(k = 1)$, are relevant. For the calculation of the weighted velocities, we use a special representation of $v_t(m)$.

The dependency of the fall speeds of individual ice crystals on the crystal mass is approximated by a simple power law $v_t(m) = \gamma m^\delta \mathrm{corr}(T,p)$, including a temperature and pressure dependent density correction factor,

$$\mathrm{corr}(T,p) = \left(\frac{p}{p_{00}}\right)^{a_i} \left(\frac{T}{T_{00}}\right)^{a_2}, \tag{B11}$$

with $T_{00} = 233\,\mathrm{K}$, $p_{00} = 300\,\mathrm{hPa}$, $a_1 = -0.178$, $a_2 = -0.397$. The coefficients $\gamma = 63292.36\,\mathrm{ms}^{-1}\mathrm{kg}^{-\delta}$ and $\delta = 0.57$ are assumed to be constant over the entire range of m, as opposed to piece wise constant values in Spichtinger and Gierens (2009) . This approximation is justified since we assume ice crystals of sizes in the range between $\sim 10\,\mu\mathrm{m}$ and $\sim 200\,\mu\mathrm{m}$ for SVCs. The weighted velocities for number and mass flux, respectively, have the following form:

$$\bar{v}_0 = \bar{v}_n = \gamma \frac{\mu_\delta}{\mu_0} \cdot \mathrm{corr}(T,p), \quad \bar{v}_1 = \bar{v}_q = \gamma \frac{\mu_{\delta+1}}{\mu_1} \cdot \mathrm{corr}(T,p). \tag{B12}$$

Coefficients

For simplification of the representation of the main system, we introduced coefficients in equations (25). In the following the coefficients are provided.

$$a = \frac{4}{3}\pi N_a \mu_{3,a}[r] \tag{B13a}$$

$$b = \frac{\gamma}{\Delta z} c(T,p) r_0^{\frac{\delta(\delta-1)}{2}} \tag{B13b}$$

$$c = \frac{\gamma}{\Delta z} c(T,p) r_0^{\frac{\delta(\delta+1)}{2}} \tag{B13c}$$

$$d = \frac{4}{3}\pi C_i \varepsilon \rho D_v \frac{p_{si}(T)}{p} r_0^{\frac{\alpha_i(\alpha_i-1)}{2}} \frac{1}{100\%} \tag{B13d}$$

$$e = g\frac{M_{air}}{RT}\left(\frac{L_{ice}}{c_p T} - 1\right) \tag{B13e}$$

$$f = \frac{4}{3}\pi C_i \varepsilon \rho D_v r_0^{\frac{\alpha_i(\alpha_i-1)}{2}} \tag{B13f}$$

Appendix C: Derivation of eq. (28)

For deriving equation (28) we start with the slightly simplified systems of equations:

$$a \cdot J(RH_i, T) - b \cdot N_c^{1-\delta} q_c^{\delta} = 0 \tag{C1a}$$

$$-c \cdot N_c^{-\delta} q_c^{\delta-1} + d \cdot (RH_i - 100\%) N_c^{1-\alpha_i} q_c^{\alpha_i} = 0 \tag{C1b}$$

$$e \cdot w \cdot RH_i - f \cdot (RH_i - 100\%) N_c^{1-\alpha_i} q_c^{\alpha_i} = 0 \tag{C1c}$$

We convert equation (C1b) into the following form, using the mean mass $\overline{m} = q_c/N_c$ for cloudy states ($N_c \neq 0$):

$$-c \cdot \overline{m}^{\delta} + d \cdot (RH_i - 100\%) \overline{m}^{\alpha_i - 1} = 0. \tag{C2}$$

From this equation we obtain a representation for the mean mass:

$$\overline{m} = \left(\frac{d}{c}(RH_i - 100\%)\right)^{\frac{1}{\delta+1-\alpha_i}}. \tag{C3}$$

In a similar way, we can rearrange equation (C1a) for a representation of N_c:

$$N_c = \frac{a \cdot J(RH_i, T)}{b} \cdot \overline{m}^{-\delta}. \tag{C4}$$

Using equations (C3) and (C4) in equation (C1c) we obtain equation (28). The roots w.r.t. RH_i of this equation are calculated using Newton's method.

Appendix D: Example for a Poincaré section

In figure 16 we present an example of a Poincaré section, as used for the determination of the limit cycle. The plane, Σ, is such that RH_i is constant on Σ and $\boldsymbol{x}_0$ is in ~~large-scale models; since these models describe the structure of clouds in terms of cloud variables and environmental conditions, these models might be used for describing such structures embedded into a coarse grid model. However, further research in this direction is necessary in order to proceed from pure model prototypes to meaningful cloud parameterisations~~Σ. Two different scenarios are represented here. First, we use a point close to the unstable focus point as initial condition for the numerical integration (indicated by red cross). The red dots indicate the section of the trajectory with the transversal plane Σ. The red dots converge fast to two accumulation points, which determine approximately the section of the limit cycle with the plane Σ. If we start "outside" of the limit cycle, the section points (indicated by blue dots) again converge fast to the same two accumulation points.

Acknowledgements. We thank M. Baumgartner, M. C. ~~Götze~~Papke, L. Grüne and R. Klein for fruitful discussions. This study was prepared with support by the German "Bundesministerium für Bildung und Forschung (BMBF)" within the HD(CP)^2 initiative, project S4 (01LK1216A) and with support by the German Research Foundation (DFG) within the ~~TransRegio 165~~ Transregional Collaborative research Center TRR165 "waves to weather", project A2~~(SP 1163/6-1)~~.

References

Argyris, J., Faust, G., Haase, M., and Friedrich, R.: Die Erforschung des Chaos, Springer, Heidelberg, Germany, 2010.

aufm Kampe, H. J. and Weickmann, H. K.: The effectiveness of natural and artificial aerosols as freezing nuclei, Journal of Meteorology, 8, 283–288, 1951.

Beheng, K. D.: The Evolution of Raindrop Spectra: A Review of Microphysical Essentials., in: Rainfall: State of the Science., edited by Testik, F. Y. and Gebremichael, M., vol. 191 of *Geophysical Monograph Series*, pp. 29–48, American Geophysical Union, Washington, USA, doi:10.1029/2010GM000957, 2010.

Chen, T., Rossow, W. B., and Zhang, Y.: Radiative effects of cloud-type variations, Journal of climate, 13, 264–286, doi:10.1175/1520-0442(2000)013<0264:REOCTV>2.0.CO;2, 2000.

Davis, S., Hlavka, D., Jensen, E., Rosenlof, K., Yang, Q., Schmidt, S., Borrmann, S., Frey, W., Lawson, P., Voemel, H., and Bui, T. P.: In situ and lidar observations of tropopause subvisible cirrus clouds during TC4, Journal of Geophysical Research: Atmospheres, 115, D00J17, doi:10.1029/2009JD013093, 2010.

Dufour, L.: Ueber das Gefrieren des Wassers und über die Bildung des Hagels, Annalen der Physik, 190, 530–554, 1861.

Feingold, G. and Koren, I.: A model of coupled oscillators applied to the aerosol–cloud–precipitation system, Nonlinear Processes in Geophysics, 20, 1011–1021, 2013.

Feller, W.: An Introduction to Probability Theory and Its Applications, no. Bd. 2 in An Introduction to Probability Theory and Its Applications, Wiley, Chichester, UK, 1971.

Froyd, K., Murphy, D., Lawson, P., Baumgardner, D., and Herman, R.: Aerosols that form subvisible cirrus at the tropical tropopause, Atmospheric Chemistry and Physics, 10, 209–218, 2010.

Fu, Q. and Liou, K. N.: Parameterization of the Radiative Properties of Cirrus Clouds, Journal of the Atmospheric Sciences, 50, 2008–2025, 1993.

Hauf, T.: Microphysical kinetics in phase space: The warm rain process, Atmospheric Research, 29, 55 – 84, doi:10.1016/0169-8095(93)90037-O, 1993.

Hindmarsh, A. C.: ODEPACK, A Systematized Collection of ODE Solvers, in: Scientific Computing, edited by Stepleman, R. S., pp. 55.–64, North-Holland, 1983.

Hoareau, C., Keckhut, P., Noel, V., Chepfer, H., and Baray, J.-L.: A decadal cirrus clouds climatology from ground-based and spaceborne lidars above the south of France (43.9° N–5.7° E), Atmospheric Chemistry and Physics, 13, 6951–6963, 2013.

Hoose, C. and Möhler, O.: Heterogeneous ice nucleation on atmospheric aerosols: a review of results from laboratory experiments, Atmospheric Chemistry and Physics, 12, 9817–9854, doi:10.5194/acp-12-9817-2012, 2012.

Hosler, C. L.: On the crystallization of supercooled clouds, Journal of Meteorology, 8, 326–331, 1951.

Hulburt, H. and Katz, S.: Some problems in particle technology: A statistical mechanical formulation, Chemical Engineering Science, 19, 555–574, 1964.

Höller, H.: Parameterization of cloud-microphysical processes in a three-dimensional convective mesoscale model, Tech. rep., Deutsche Forschungs- und Versuchsanstalt für Luft- und Raumfahrt, 1986.

Immler, F., Krüger, K., Fujiwara, M., Verver, G., Rex, M., and Schrems, O.: Correlation between equatorial Kelvin waves and the occurrence of extremely thin ice clouds at the tropical tropopause, Atmospheric Chemistry and Physics, 8, 4019–4026, doi:10.5194/acp-8-4019-2008, 2008a.

Immler, F., Treffeisen, R., Krüger, K., and Schrems, O.: Cirrus, contrails, and ice supersaturated regions in high pressure systems at northern mid latitudes, Atmospheric Chemistry and Physics, 8, 1689–1699, 2008b.

Jeffreys, H.: Some Problems of Evaporation, The London, Edinburgh, and Dublin Philosophical Magazine and Journal of Science, 35, 270–280, 1918.

Jensen, E. J., Toon, O. B., Vay, S. A., Ovarlez, J., May, R., Bui, T. P., Twohy, C. H., Gandrud, B. W., Pueschel, R. F., and Schumann, U.: Prevalence of ice-supersaturated regions in the upper troposphere: Implications for optically thin ice cloud formation, Journal of Geophysical Research: Atmospheres, 106, 17 253–17 266, doi:10.1029/2000JD900526, 2001.

Kärcher, B.: Properties of subvisible cirrus clouds formed by homogeneous freezing, Atmospheric Chemistry and Physics, 2, 161–170, 2002.

Kärcher, B. and Lohmann, U.: A parameterization of cirrus cloud formation: Homogeneous freezing including effects of aerosol size, Journal of Geophysical Research, 107, 4010, doi:10.1029/2001JD000470, 2002.

Kärcher, B. and Solomon, S.: On the composition and optical extinction of particles in the tropopause region, Journal of Geophysical Research: Atmospheres, 104, 27 441–27 459, doi:10.1029/1999JD900838, 1999.

Kay, J. E., Baker, M., and Hegg, D.: Microphysical and dynamical controls on cirrus cloud optical depth distributions, Journal of Geophysical Research: Atmospheres, 111, doi:10.1029/2005JD006916, d24205, 2006.

Kemppi, M. L. and Sinclair, V. A.: Structure of a warm front: Helsinki testbed observations and model simulation, Monthly Weather Review, 139, 2876–2900, 2011.

Koop, T.: Homogeneous ice nucleation in water and aqueous solutions, Zeitschrift für Physikalische Chemie/International journal of research in physical chemistry and chemical physics, 218, 1231–1258, 2004.

Koop, T., Luo, B., Biermann, U. M., Crutzen, P. J., and Peter, T.: Freezing of $HNO_3/H_2SO_4/H_2O$ Solutions at Stratospheric Temperatures: Nucleation Statistics and Experiments, Journal of Physical Chemistry A, 101, 1117–1133, 1997.

Koop, T., Luo, B., Tsias, A., and Peter, T.: Water activity as the determinant for homogeneous ice nucleation in aqueous solutions, Nature, 406, 611–614, 2000.

Koren, I. and Feingold, G.: Aerosol–cloud–precipitation system as a predator-prey problem, Proceedings of the National Academy of Sciences, 108, 12 227–12 232, 2011.

Krämer, M., Rolf, C., Luebke, A., Afchine, A., Spelten, N., Costa, A., Meyer, J., Zöger, M., Smith, J., Herman, R. L., Buchholz, B., Ebert, V., Baumgardner, D., Borrmann, S., Klingebiel, M., and Avallone, L.: A microphysics guide to cirrus clouds – Part 1: Cirrus types, Atmospheric Chemistry and Physics, 16, 3463–3483, 2016.

Kübbeler, M., Hildebrandt, M., Meyer, J., Schiller, C., Hamburger, T., Jurkat, T., Minikin, A., Petzold, A., Rautenhaus, M., Schlager, H., Schumann, U., Voigt, C., Spichtinger, P., Gayet, J., Gourbeyre, C., and Krämer, M.: Thin and subvisible cirrus and contrails in a subsaturated environment, Atmos. Chem. Phys, 11, 5853–5865, 2011.

Lamb, D. and Verlinde, J.: Physics and Chemistry of Clouds, Cambridge University Press, Cambridge, UK, 2011.

Lawson, R. P., Pilson, B., Baker, B., Mo, Q., Jensen, E., Pfister, L., and Bui, P.: Aircraft measurements of microphysical properties of subvisible cirrus in the tropical tropopause layer, Atmospheric Chemistry and Physics, 8, 1609–1620, doi:10.5194/acp-8-1609-2008, 2008.

Luebke, A. E., Afchine, A., Costa, A., Grooß, J.-U., Meyer, J., Rolf, C., Spelten, N., Avallone, L. M., Baumgardner, D., and Krämer, M.: The origin of midlatitude ice clouds and the resulting influence on their microphysical properties, Atmospheric Chemistry and Physics, 16, 5793–5809, doi:10.5194/acp-16-5793-2016, 2016.

McDonald, J.: Use of the electrostatic analogy in studies of ice crystal growth, Zeitschrift für angewandte Mathematik und Physik, 14, 610–620, doi:10.1007/BF01601268, 1963.

Minikin, A., Petzold, A., Ström, J., Krejci, R., Seifert, M., van Velthoven, P., Schlager, H., and Schumann, U.: Aircraft observations of the upper tropospheric fine particle aerosol in the Northern and Southern Hemispheres at midlatitudes, Geophysical Research Letters, 30, 1503, doi:10.1029/2002GL016458, 2003.

Murphy, D. and Koop, T.: Review of the vapour pressures of ice and supercooled water for atmospheric applications, Quarterly Journal of the Royal Meteorological Society, 131, 1539–1565, 2005.

Oreskes, N.: The role of quantitative models in science, in: Models in Ecosystem Science, edited by Canham, C. D., Cole, J. J., and Lauenroth, W. K., pp. 13–31, Princeton University Press, 2003.

Oreskes, N., Shrader-Frechette, K., and Belitz, K.: verification, validation and confirmation of numerical models in Earth sciences, Science, 263, 641–646, 1994.

Pruppacher, H. R. and Klett, J. D.: Microphysics of clouds and precipitation, Kluwer Acad. Pub., Dordrecht, 1997.

Ramkrishna, D.: Population Balances, Academic Press, New York, USA, 2000.

Ren, C. and Mackenzie, A. R.: Cirrus parametrization and the role of ice nuclei, Quarterly Journal of the Royal Meteorological Society, 131, 1585–1605, doi:10.1256/qj.04.126, 2005.

Sassen, K. and Campbell, J. R.: A midlatitude cirrus cloud climatology from the Facility for Atmospheric Remote Sensing. Part I: Macrophysical and synoptic properties, Journal of the atmospheric sciences, 58, 481–496, 2001.

Sassen, K. and Dodd, G. C.: Haze particle nucleation simulations in cirrus clouds, and applications for numerical and lidar studies, Journal of the Atmospheric Sciences, 46, 1989.

Seifert, A. and Beheng, K.: A two-moment cloud microphysics parameterization for mixed-phase clouds. Part 1: Model description, Meteorology and atmospheric physics, 92, 45–66, 2006.

Seifert, P., Ansmann, A., Müller, D., Wandinger, U., Althausen, D., Heymsfield, A. J., Massie, S. T., and Schmitt, C.: Cirrus optical properties observed with lidar, radiosonde, and satellite over the tropical Indian Ocean during the aerosol-polluted northeast and clean maritime southwest monsoon, Journal of Geophysical Research: Atmospheres, 112, 2007.

Spichtinger, P. and Cziczo, D. J.: Impact of heterogeneous ice nuclei on homogeneous freezing events in cirrus clouds, Journal of Geophysical Research, 115, 2010.

Spichtinger, P. and Gierens, K. M.: Modelling of cirrus clouds–Part 1a: Model description and validation, Atmospheric Chemistry and Physics, 9, 685–706, 2009.

Stephens, G. L.: The influence of radiative transfer on the mass and heat budgets of ice crystals falling in the atmosphere, Journal of the Atmospheric Sciences, 40, 1729–1739, 1983.

Stocker, T., Qin, D., Plattner, G.-K., Tignor, M., Allen, S., Boschung, J., Nauels, A., Xia, Y., Bex, V., and Midgley, P., eds.: IPCC, 2013: Climate Change 2013: The Physical Science Basis. Contribution of Working Group I to the Fifth Assessment Report of the Intergovernmental Panel on Climate Change, Cambridge University Press, Cambridge, United Kingdom and New York, NY, USA, 2013.

Stubenrauch, C. J., Cros, S., Guignard, A., and Lamquin, N.: A 6-year global cloud climatology from the Atmospheric InfraRed Sounder AIRS and a statistical analysis in synergy with CALIPSO and CloudSat, Atmospheric Chemistry and Physics, 10, 7197–7214, doi:10.5194/acp-10-7197-2010, 2010.

Turing, A. M.: The Chemical Basis of Morphogenesis, Philosophical Transactions of the Royal Society of London. Series B, Biological Sciences, 237, 37–72, 1952.

Verhulst, F.: Nonlinear differential equations and dynamical systems, Springer, Heidelberg, Germany, 2 edn., 1996.

Wacker, U.: Structual stability in cloud physics using parameterized microphysics, Beiträge zur Physik der Atmosphäre, 65, 231–242, 1992.

Wacker, U.: Competition of Precipitation Particles in a Model with Parameterized Cloud Particles, J. Atmos. Sci., 52, 2577–2589, 1995.

Wacker, U.: Nonlinear effects in a conceptual multilayer cloud model, Nonlinear Processes in Geophysics, 13, 99–107, doi:10.5194/npg-13-99-2006, 2006.

Wang, P.-H., Minnis, P., McCormick, M. P., Kent, G. S., and Skeens, K. M.: A 6-year climatology of cloud occurrence frequency from Stratospheric Aerosol and Gas Experiment II observations (1985–1990), Journal of Geophysical Research, 101, 29 407–29 429, 1996.

Weigel, R., Spichtinger, P., Mahnke, C., Klingebiel, M., Afchine, A., Petzold, A., Krämer, M., Costa, A., Molleker, S., Jurkat, T., Minikin, A., , and Borrmann, S.: Thermodynamic correction of particle concentrations measured by underwing probes on fast flying aircraft, Atmospheric Measurement Techniques Discussions, 8, 13 423–13 469, doi:10.5194/amtd-8-13423-2015, 2015.

Wernli, H., Boettcher, M., Joos, H., Miltenberger, A. K., and Spichtinger, P.: A trajectory-based classification of ERA-Interim ice clouds in the region of the North Atlantic storm track, Geophysical Research Letters, 43, 6657–6664, 2016.

Zhang, Y., Macke, A., and Albers, F.: Effect of crystal size spectrum and crystal shape on stratiform cirrus radiative forcing, Atmospheric Research, 52, 59–75, 1999.

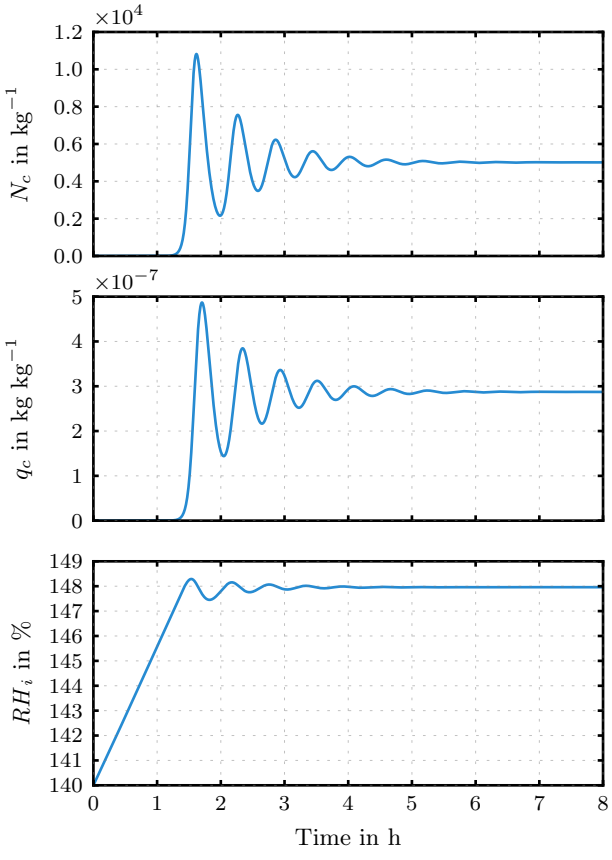

Figure 1. ~~Here, a~~ A scenario in state 1 (~~damping~~point attractor regime, damped) ~~is shown~~ at ~~$w = 0.01\,\mathrm{ms}^{-1}$~~ $w = 0.01\,\mathrm{m\,s}^{-1}$ and $T = 220\,\mathrm{K}$. The continuous nucleation as well as similar time scales of nucleation, growth and sedimentation lead to a damped oscillation with an equilibrium state for $t > 7$ h. In ~~the~~ phase space, the attractor property is ~~visible~~ more obvious (see figure 5).

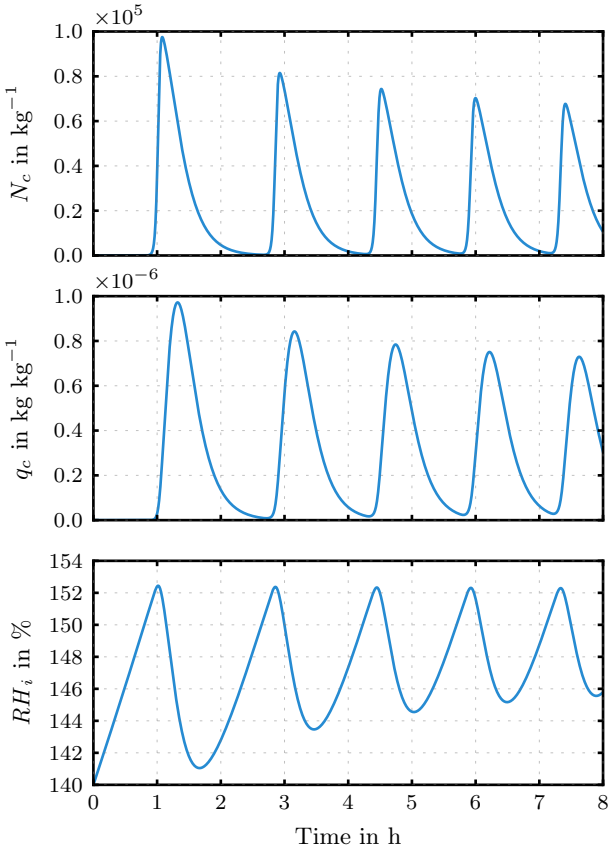

Figure 2. ~~Here, a~~ A scenario in state 2 (limit cycle regime) is shown at ~~$w = 0.02\,\mathrm{ms}^{-1}$~~ $w = 0.02\,\mathrm{m\,s}^{-1}$ and $T = 210\,\mathrm{K}$. Nucleation events occur as pulses, thus an undamped oscillation evolves, which describes a limit cycle in ~~the~~ phase space (see figure 6).~~)~~

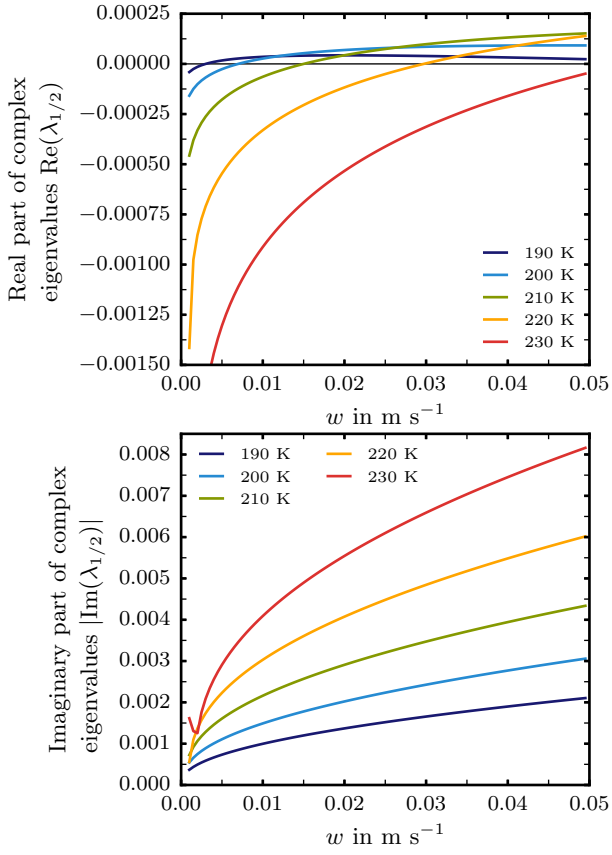

Figure 3. Real (upper panel) and imaginary part (lower panel) of the complex eigenvalues $\lambda_{1,2}$ of the Jacobian $\mathbf{DF}|_{\boldsymbol{x}_0}$ at the equilibrium point $\boldsymbol{x}_0$.

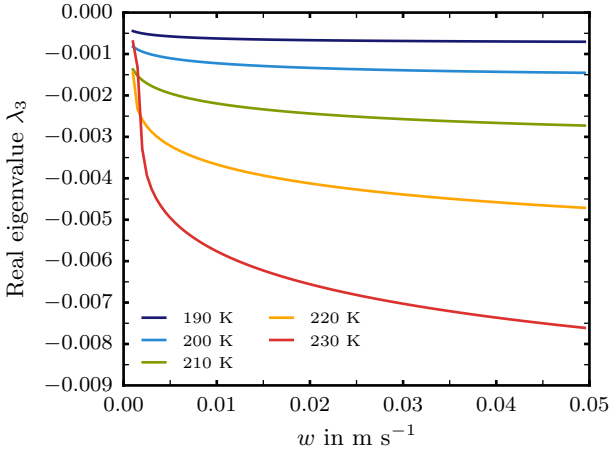

Figure 4. Real eigenvalue λ_3 of the Jacobian $\mathbf{DF}|_{\boldsymbol{x}_0}$ at the equilibrium point $\boldsymbol{x}_0$.

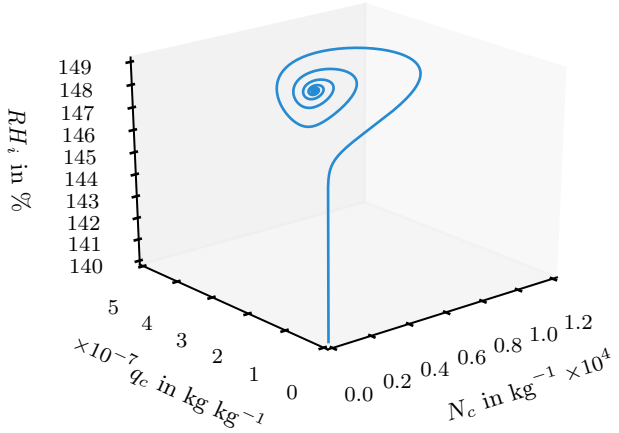

Figure 5. Positive point attractor for state 1 at $T = 220\,\mathrm{K}$, ~~$w = 0.01\,\mathrm{ms}^{-1}$~~ $w = 0.01\,\mathrm{m\,s}^{-1}$: orbit in ~~the~~ phase space approaching the equilibrium point.

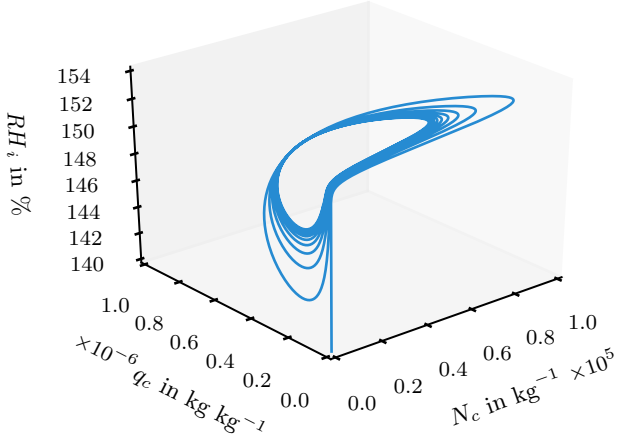

Figure 6. Limit cycle for state 2: orbit in ~~the~~ phase space at $T = 210\,\mathrm{K}$, ~~$w = 0.02\,\mathrm{ms}^{-1}$~~ $w = 0.02\,\mathrm{m\,s}^{-1}$. Note that the solution starts "outside" of the limit cycle and approaches the limit cycle attractor asymptotically.

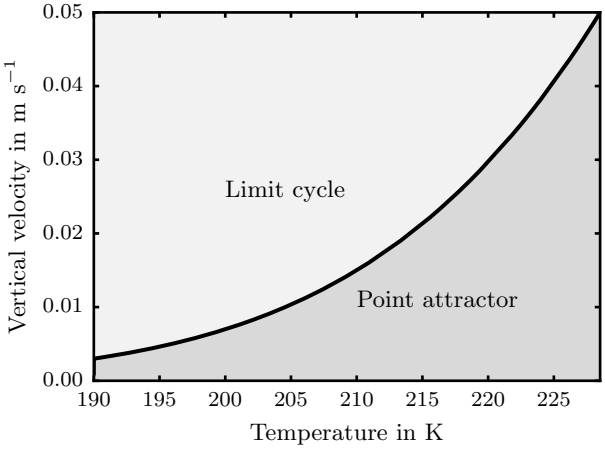

Figure 7. Bifurcation diagram for “positive point attractor" (state 1) and “limit cycle" (state 2) regimes in the w-T-space. The thick line indicates the location of the Hopf bifurcation.

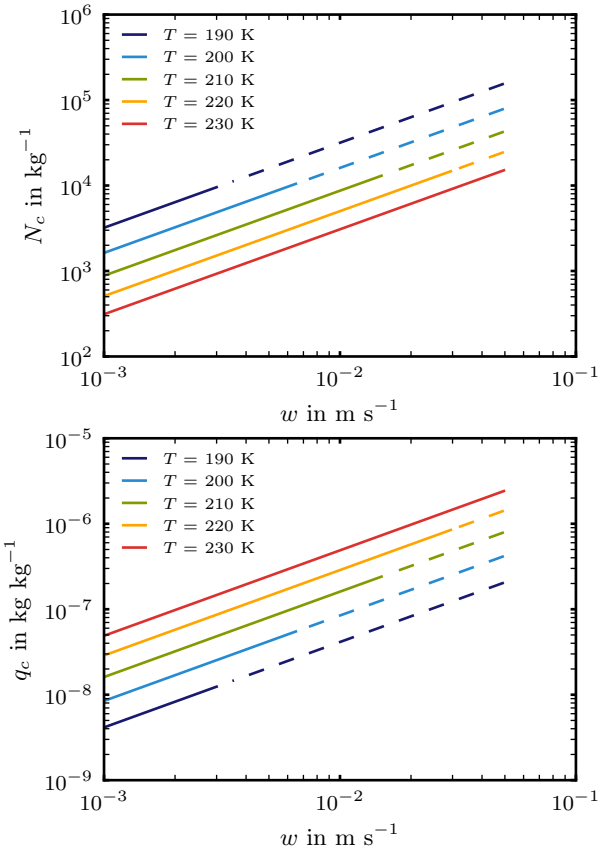

Figure 8. Ice particle number concentration N_c (upper panel) and ice particle mass concentration q_c (lower panel) at the critical point as a function of vertical velocity for different temperatures. Solid lines ~~are for~~ indicate parameter combinations (w, T) in the point attractor regime (state 1), dashed lines ~~are for~~ represent the limit cycle regime (state 2).

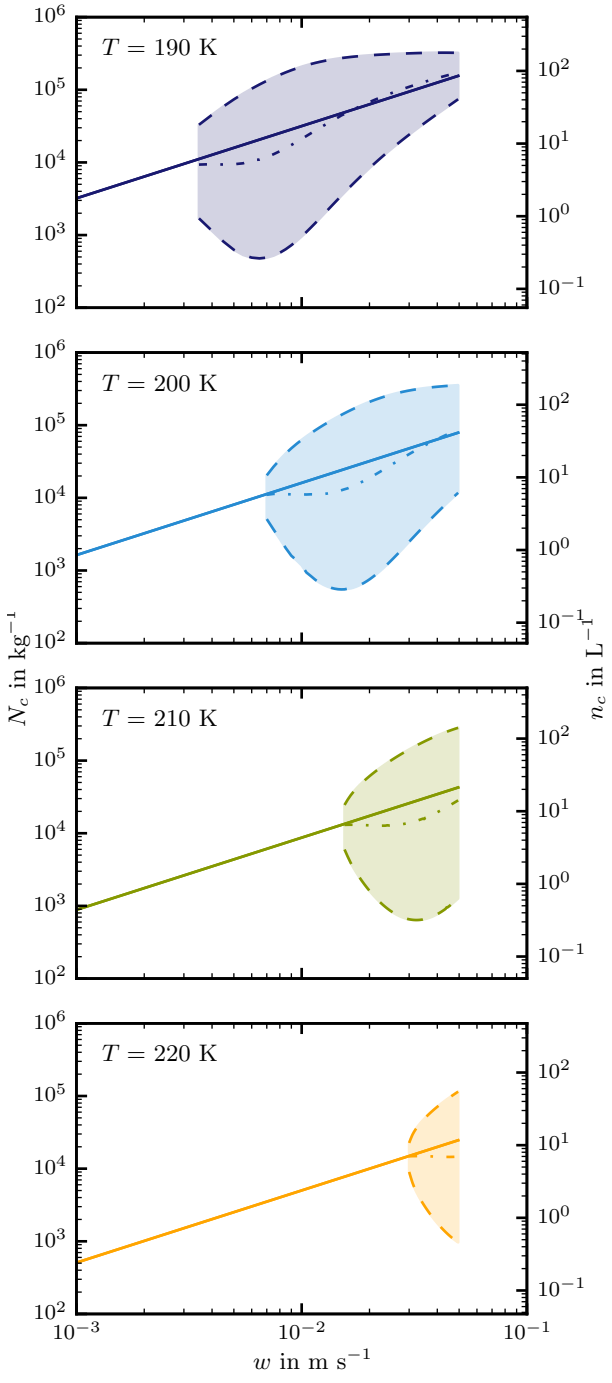

Figure 9. Ice crystal number concentrations for different temperature scenarios ($T = 190, 200, 210, 220\,\mathrm{K}$). The solid line represents values at the critical point $\boldsymbol{x}_0$ (stable or unstable focus). For the limit cycle regime the range of ice crystal number concentrations is indicated by the shaded area bounded by minimum and maximum values for the updraught range ~~$0.001 \leq w \leq 0.05\,\mathrm{ms}^{-1}$~~ $0.001 \leq w \leq 0.05\,\mathrm{m\,s}^{-1}$; the median is indicated by the ~~dashed~~ dot-dashed line.

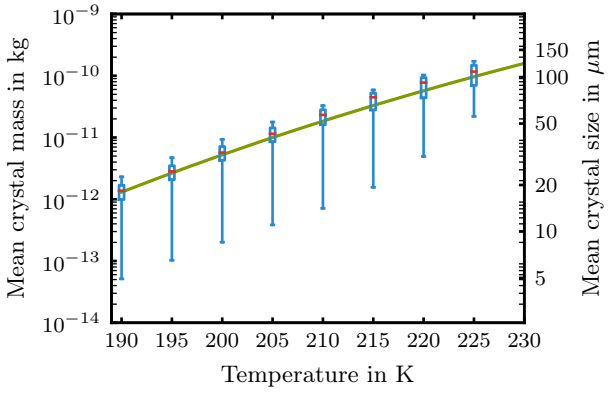

Figure 10. Mean ice crystal mass $\overline{m}$ as a function of temperature. For the critical point $\boldsymbol{x}_0$, values of $\overline{m}$ depends only slightly on the vertical velocity, the curve covers the area that corresponds to vertical velocities ~~$0.001\,\mathrm{m\,s^{-1}} \leq w \leq 0.05\,\mathrm{m\,s^{-1}}$~~ $0.001\,\mathrm{m\,s^{-1}} \leq w \leq 0.05\,\mathrm{m\,s^{-1}}$. Additionally, box and whiskers plots indicate median, 25%~~,~~/ 75% percentiles, and minimum/maximum values, respectively, for the limit cycle regime.

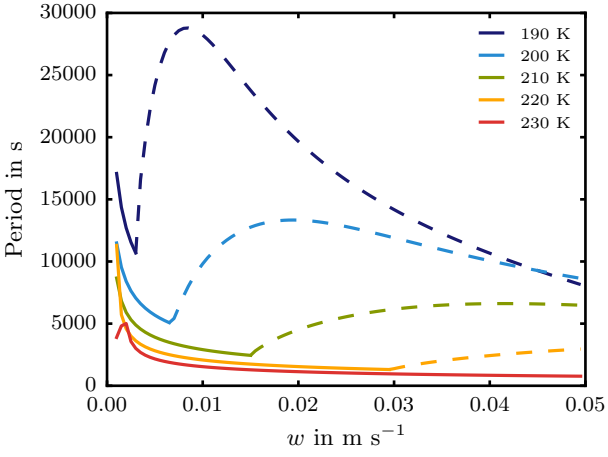

Figure 11. Oscillation periods for the point attractor regime at $\boldsymbol{x}_0$ (solid lines), and for the limit cycle regime (dashed lines).

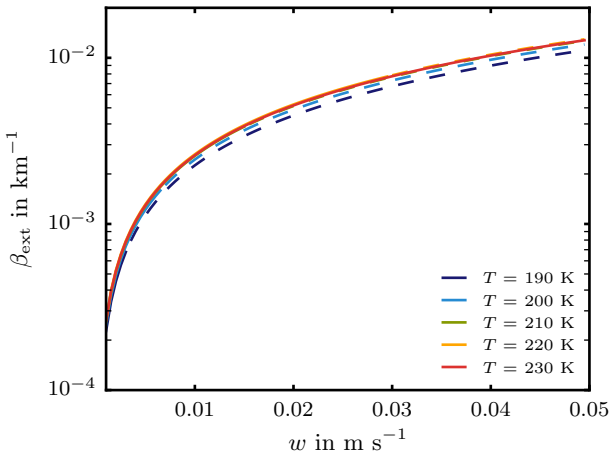

Figure 12. Extinction coefficient at $\boldsymbol{x}_0$ for different temperatures in point attractor state 1 (solid lines) and limit cycle state 2 (dashed lines).

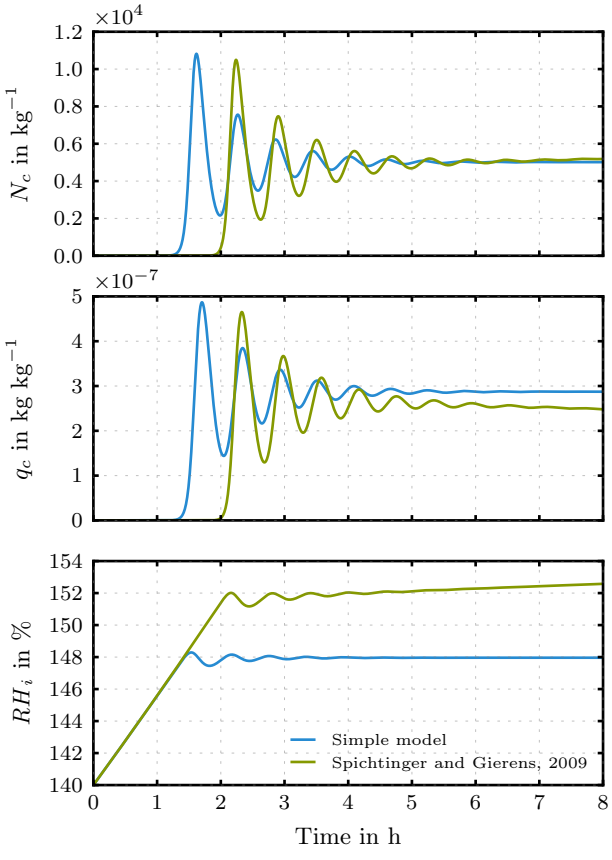

Figure 13. ~~Attractor~~ Point attractor case (state 1): Comparison between simple box model and the complex model by Spichtinger and Gierens (2009). ~~$w = 0.01\text{ms}^{-1}$~~ Updraught $w = 0.01\,\text{m s}^{-1}$, temperature in the simple model and start temperature of the complex model is $T = 220\,\text{K}$.

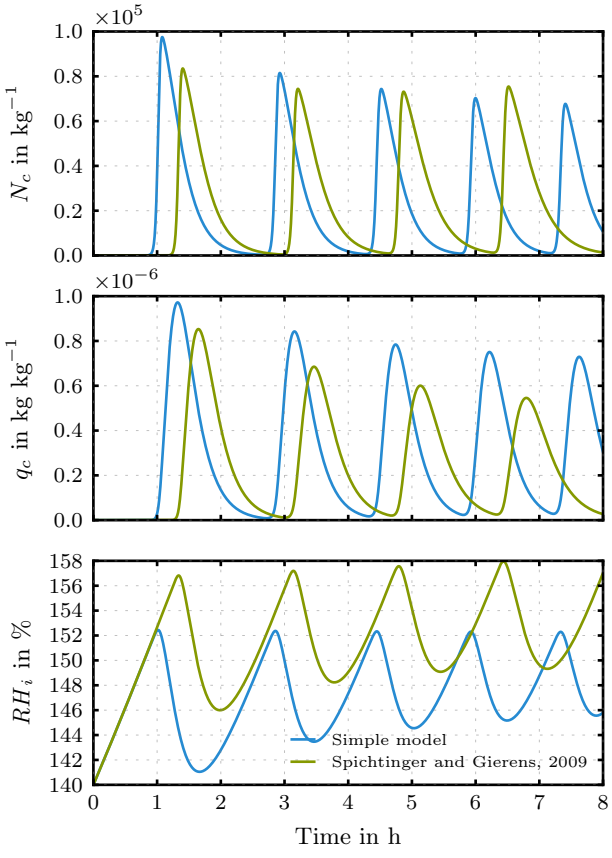

Figure 14. Limit cycle case (state 2): Comparison between simple box model and the complex model by Spichtinger and Gierens (2009). ~~$w = 0.02\,\mathrm{ms}^{-1}$~~ Updraught $w = 0.02\,\mathrm{m\,s}^{-1}$, temperature in the simple model and start temperature of the complex model is $T = 210\,\mathrm{K}$.

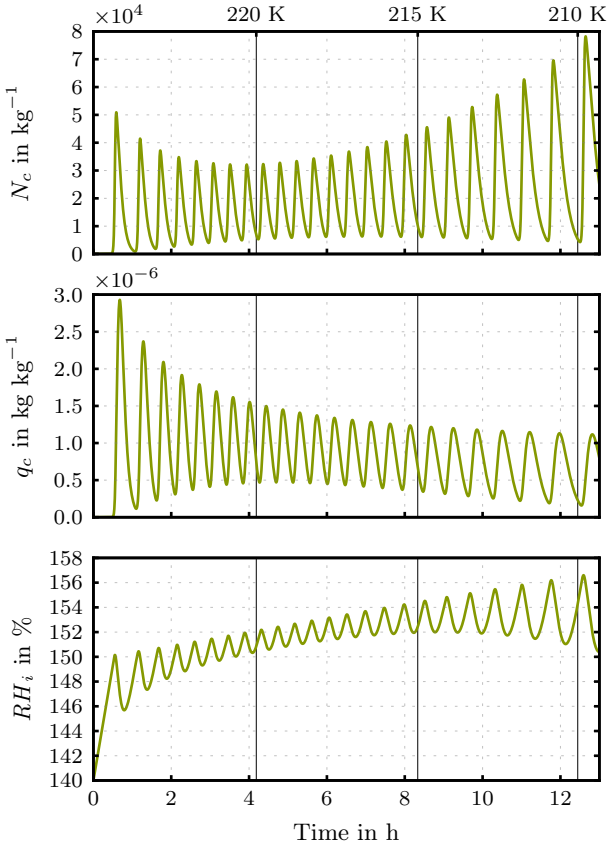

Figure 15. Transition between attractor regime (state 1) and limit cycle regime (state 2): Simulation with the complex model by Spichtinger and Gierens (2009) for ~~$w = 0.035\mathrm{ms}^{-1}$~~ $w = 0.035\,\mathrm{m\,s}^{-1}$ and start temperature: $T = 225\,\mathrm{K}$. During the first two hours of ~~simulations~~the simulation, the attractor characteristics can be clearly seen. After reaching temperatures of about $T \sim 220\,\mathrm{K}$, the regime changes from state 1 (point attractor) to state 2 (limit cycle), see also phase diagram in fig. 7. ~~after~~ After this transition, the amplitudes of number concentrations and relative humidity w.r.t. ice increase and at the end of the simulation also a shift in the oscillation period can be seen. Increase in amplitude and shift in oscillation period are due to changes of the limit cycle properties for decreasing temperature ~~change~~(see, e.g., figure 11)

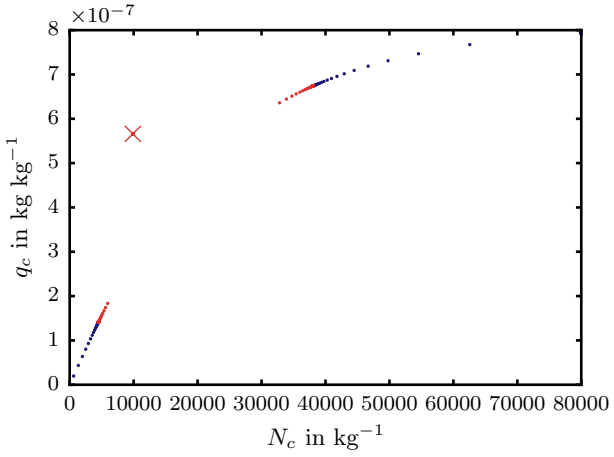

Figure 16. Example of a Poincaré section in the limit cycle regime. Blue dots indicate intersection points of the trajectory with Σ when starting "outside" the cycle, red dots indicate intersection points when starting near the (unstable) equilibrium point $\boldsymbol{x}_0$ (red cross).